7

Deep-Water Variability and Interbasin Interactions in the Eastern Mediterranean Sea

Emin Özsoy[1], Sarantis Sofianos[2], Isaac Gertman[3], Anneta Mantziafou[2], Ali Aydoğdu[1], Sotiria Georgiou[2], Ersin Tutsak[1], Alex Lascaratos[2], Artur Hecht[3], and Mohammed Abdul Latif[1]

7.1. INTRODUCTION

Ocean–atmosphere-land interactions and consequent feedbacks between regional and global climate systems, could be disproportionately large in the Mediterranean as a result of contrasts between marine and continental climates and complex land-sea bottom topography [*Özsoy*, 1999]. The eastern basin of the Mediterranean is a remote area of the world ocean, the isolation of its various basins increased with distance from the Atlantic Ocean and with further constraints posed by the various straits.

The eastern Mediterranean and especially its easternmost basin, the Levantine Sea, were less well known in the first half of the last century, especially when compared with the western basin, though rapidly became the subject of advanced studies carried out since the Physical Oceanography of the Eastern Mediterranean [*POEM Group*, 1992] research program of 1985–1991. Despite continuing efforts under national and international programs, there appears to be a greater need for systematic observations in the whole of the eastern Mediterranean to understand its high level of climatic variability [*Özsoy*, 1999; *Lionello et al.*, 2006; *Hoepffner*, 2006; *CIESM*, 2008, 2011; *Malanotte-Rizzoli and the Pan-Med Group*, 2012].

The investigation of the deep-water characteristics and their variability on long timescales can help in the understanding of the possible mechanisms, sensitivity, localization, and frequency of water mass formation, and their links to atmospheric forcing. The need to document and understand deep-water variability is especially acute in the case of the eastern Mediterranean Sea, where unexpected recent changes have been observed in the thermohaline transport components connected with multiple sites of intermediate and deep convection.

The water masses in the ocean are usually identified with distinct water properties such as temperature and salinity pairs. The water masses are formed as a result of long-term circulation and mixing processes and in some way they are associated with the thermohaline circulation. For the Mediterranean basin, there are meridional and zonal vertical circulation belts. An open-ended, shallow zonal vertical circulation completes a circuit by the entry of Atlantic Water (AW) at Gibraltar, later transformed into Levantine Intermediate Water (LIW) in the eastern Mediterranean, which then returns to the Atlantic Ocean as a submerged flow. Superposed on this circulation, closed, deep meridional cells are created as a result of the deep-water mass formation in the northern parts of the Mediterranean basin (Gulf of Lions, Adriatic Sea, and Aegean Sea). The zonal cells have decadal timescales, while the meridional overturning cells have multidecadal timescales (50–80 years) [*Pinardi* and *Masetti*, 2000].

High salinity Levantine Intermediate Water (LIW) occupying the intermediate layer of the eastern Mediterranean basin (200–500 m) is formed in the permanent Rhodes Gyre [*Ovchinnikov and Plakhin*, 1984; *Lascaratos and Nittis*, 1998; *Pinardi and Masetti*, 2000; *LIWEX Group*, 2003], along the adjacent zones of the

[1] *Institute of Marine Sciences, METU, Erdemli, Mersin, Turkey*
[2] *University of Athens, Athens, Greece*
[3] *Israel Oceanographic and Limnological Research, Haifa, Israel*

The Mediterranean Sea: Temporal Variability and Spatial Patterns, Geophysical Monograph 202. First Edition.
Edited by Gian Luca Eusebi Borzelli, Miroslav Gačić, Piero Lionello, and Paola Malanotte-Rizzoli.

southern Aegean and northern Levantine, such as the Gulf of İskenderun and often simultaneously with deep waters [*Sur et al.*, 1993; *Özsoy et al.*, 1993].

The Eastern Mediterranean Deep Water (EMDW) is characteristic water mass of the deep eastern basin. Using limited amounts of data obtained in the late 1950s early 1960s, *Pollak* [1951], *Lacombe and Tchernia* [1960], *Wüst*[1961], *Plakhin* [1972], *Miller* [1974], and *El-Gindy and El-Din* [1986] have implied the Aegean Sea as a possible source contributing to the formation of the EMDW, although it has often been suspected that the quantity and density of the Aegean outflow would not be sufficient to contribute to the EMDW.

Based on historical data obtained since early last century [*Nielsen*, 1912], followed by others around mid-century [*Wüst*, 1961], and including those obtained by the extensive coverage during the POEM program, the Adriatic Sea was widely accepted as the main source of the EMDW. According to this dominant view of the past, the dense waters formed in winter in the relatively shallow Adriatic Sea, flowed to the bottom of the Ionian Sea, and spread farther to the Levantine Sea [*Wüst*, 1961; *Schlitzer et al.*, 1991; *Malanotte-Rizzoli and Hecht*, 1988]. The deep-water overturning time was estimated roughly to be about 100 years with an average formation rate of 0.3 Sv (1 Sverdrup = 10^6 m^3 s^{-1}) [*Roether et al.*, 1991].

Major changes in the deep-water formation and renewal occurred in the 1990s, when it became evident that the Aegean Sea acted as a new source of EMDW, instead of the widely held view on its Adriatic Sea origin. The first signs came during the *Meteor* cruise M25 of 1993, when an anomalously saline, warm-water mass was found in the deep Levantine Sea [*Heike et al.*, 1994]. The hydrographic surveys of 1994–1995 further revealed the Aegean Sea as a dominant source of deep water [*Roether et al.*, 1996, 2007; *Klein et al.*, 1999; *Lascaratos et al.*, 1999; *Malanotte-Rizzoli et al.*, 2003]. The average outflow rate from the Cretan Basin of the new deep water formed in the Aegean Sea was estimated to be about 1.2 Sv [*Roether et al.*, 1996], and later the estimate was revised to be about 3.0 Sv during the peak outflow period between 1992 and 1994 [*Roether et al.*, 2007], much greater than the former Adriatic outflow rate.

The mechanism creating the Cretan Dense Water (CDW) filling the Cretan Basin before its outflow to the eastern basin was not very well documented, although it was suspected that consecutive transformations between the shallow shelf area and the three deep basins of the Aegean Sea resulted in dense water flowing south from the northern reaches of the sea. Higher salinities and increased amounts of LIW entering the Aegean Sea from the Levantine Basin [*Malanotte-Rizzoli et al.*, 1999; Theocharis et al., 1999; *Zervakis and Georgopoulos*, 2002] aiding shelf mixing at the Samothraki and Lemnos plateaus of the north Aegean [*Ovchinnikov et al.*, 1990; *Theocharis and Georgopoulos*, 1993; *Lascaratos et al.*, 1999; *Zervakis et al.*, 2000a] and potentially at the Cyclades plateau of the central Aegean [*Theocharis et al.*, 1999; *Gertman et al.*, 2006] created the dense waters finally reaching the Cretan Basin. The dense water formed in the upper reaches of the Aegean Sea eventually fills the deep Cretan Sea Basin and results in outflows through the Cretan Sea Straits, triggering the EMT events. *Zervakis et al.* [2003] and *Androulidakis et al.* [2012] show that the air-sea interactions and lateral inputs of the low-density Black Sea Water (BSW) outflowing from the Dardanelles Strait can effectively modulate the dense-water production in the north Aegean Sea.

In about the same years that the main part of the POEM program was concluded, it had become clear through new observations that significant changes were taking place in the eastern Mediterranean. In the northeastern part of the sea, cold winters in 1985, 1987, 1989, and 1992–1993 created favorable conditions for Levantine Intermediate Water (LIW) formation on the periphery of the Rhodes Gyre, in the northern Levantine Basin, often simultaneously with deep-water formation at the center of the Rhodes cyclonic circulation [*Özsoy et al.*, 1989, 1991, 1993; *Sur et al.*, 1993; *Gertman et al.*, 2006]. During the same years, the last common field experiment of POEM in October 1991 indicated significant changes in the thermohaline circulation. Increased salinity of the Levantine surface water in this period [*Özsoy et al.*, 1993; *Hecht and Gertman*, 2001; *Gertman et al.*, 2006] coincident with the blocking of the Levantine circulation by large anticyclonic eddies, resulted in diversion toward the Aegean Sea of the saline water transported by the Asia Minor Current (AMC) along the Anatolian coast [*Malanotte-Rizzoli et al.*, 1999; *Theocharis et al.*, 1999]. Changes in the air-sea fluxes during the same period were associated with a series of observed changes in the circulation and hydrography [*Zervakis et al.*, 2000; *Josey*, 2003].

A number of studies used numerical modeling techniques to simulate the events in an effort to understand exact sequence of the events and the underlying physics. The role of changes in the Aegean Sea atmospheric forcing [*Samuel et al.*, 1999], the dense-water formation processes in the north Aegean Sea [*Androulidakis et al.*, 2012], the mixing effects of a series of cold winters during 1987–1995 on the Cretan Sea outflow dynamics [*Wu et al.*, 2000], and the details of LIW and EMDW production near the Rhodes Gyre [*Lascaratos et al.*, 1999; *Nittis et al.*, 2003] were investigated by numerical simulations. Other numerical experiments [*Stratford and Haines*, 2002; *Beuvier et al.*, 2010] showed sensitivity to successive cold winters and changes in atmospheric forcing, resulting in dense-water outflow from the Aegean Sea.

A box-model with interbasin coupling [*Ashkenazy et al.*, 2011] showed multiple states of the nonlinear system, implying underlying instabilities.

Despite all experimental and numerical evidence, it is not yet clear how frequent is the switching between deep-water sources, or how persistent are the described thermohaline circulation cells of the Mediterranean Sea. It is also not clear how the events at near-surface or deep levels are connected to the surface climatological forcing by the atmosphere. In this study, however, we are presently not much concerned with the connection to the atmosphere, as we will only be analyzing the deep-water characteristics independent of the changes in the upper-water column.

In the following, we provide the data sources and methodology (section 2), followed by an analysis of the changes in basinwide properties linked with the interactions between individual basins of the eastern Mediterranean (section 3), and the intrabasin variability (section 4). We provide a general discussion in section 5.

7.2. METHODOLOGY

In this work, we tried to collect the most complete temperature and salinity profile dataset in the eastern Mediterranean (1912–2010). A comprehensive dataset was made available by ISRAMAR, the Israel Marine Data Center, National Institute of Oceanography of the IOLR, Israel. This dataset is based on MEDAR/MEDATLAS II collection (http://www.ifremer.fr/medar) and the MATER project collection (http://www.ifremer.fr/sismer/program/mater). Additional POEM basinwide cruises (1985–1991) obtained in several multinational cruises in the eastern Mediterranean as well as Soviet cruises (1987–1990) in the eastern Mediterranean [*Hecht and Gertman*, 2001] were included. The dataset was extended significantly by POEM and Soviet cruises data, and also in the framework of SESAME EU project, including recent cruise and ARGO floats data collected from publicly available oceanographic databases ("WOD05"— http://www.nodc.noaa.gov/OC5/WOD05/pr_wod05.html; "Coriolis" —http://www.coriolis.eu.org; "ICES"—http://ocean.ices.dk), as well as cruise data collected in the framework of the SESAME project. The data are inclusive of the SeaDataNet CTD and bottle database, except that the ISRAMAR database has the above additions with a larger number of casts and improved quality control of the data after 2000. Data obtained by bottles, CTD, and Argo floats were accepted for analysis. XBT data were rejected due to their relatively low accuracy, which is comparable with the variability in deep layers. The vertical resolution of the analyzed data varies as a function of the dates of data collection, instrument type, etc., but the CTD data available after the 1980s typically have a resolution of about 1 m.

The Mediterranean and especially the eastern Mediterranean Sea is trapped among three continents and divided into several basins by the geometry of the main landmasses and islands. Because each region in the Mediterranean has specific climate and each part of the sea responds differently to the forcing, it is required to discover these differences and to investigate whether particular changes are triggered in some regions and if later the effects are transmitted to other regions. We therefore analyze the data with respect to the subdomains designed in Figure 7.1. We base our analysis on all deep stations (deeper than 450 m) in the database, displayed in Figure 7.1a.

Although the stations shown in Figure 7.1a have been filtered for stations deeper than 450 m, few stations appear in shallower areas, apparently as a result of errors in entering coordinates in the database. In addition, it should be obvious that not all of these stations are used in the analysis because of the quality and depth intervals filtering described in the following.

To observe long-term climatic influences, we first look at the deep data. We have grouped the data according to subdomains shown in the map, and have then selected the data in depth intervals that were arbitrarily defined but at the same levels in all basins. We selected data below 450 m, that is, depths increasingly isolated from seasonal surface processes, specifically to study climatic influences. The depth intervals compared were selected to be 450–550 m, 900–1100 m, 1900–2100 m and 2900–3100 m, centered respectively at depths of 0.5, 1, 2, and 3 km. In shallower basins such as the Aegean and Adriatic seas, not all of these depth intervals had adequate amount of data, producing results only at depths centered at 0.5 and 1 km in the Adriatic Sea and at 0.5, 1, and 2 km in the Aegean Sea.

The data quality flags for the depth, temperature, and salinity values were checked and used to filter out data with unsatisfactory individual (flag value ≥ 2) or overall data quality assignments. The computed potential temperature (referenced to the surface), salinity, and potential density (referenced to the surface) data were collected in half-year time bins and the average, standard deviation, and confidence limits were calculated in each bin. The grouping of data in half-year bins allows sufficient time resolution to better detect dense-water spreading events expected at the cold part of the year, but relatively free of the seasonal signal diminished at depths below 500 m.

Average properties are represented by the data points in the time-series plots of Figure 7.2 an later, while confidence intervals of the mean estimates are shown by vertical bars. The calculation of the double-sided 95% confidence intervals of the estimated mean properties in

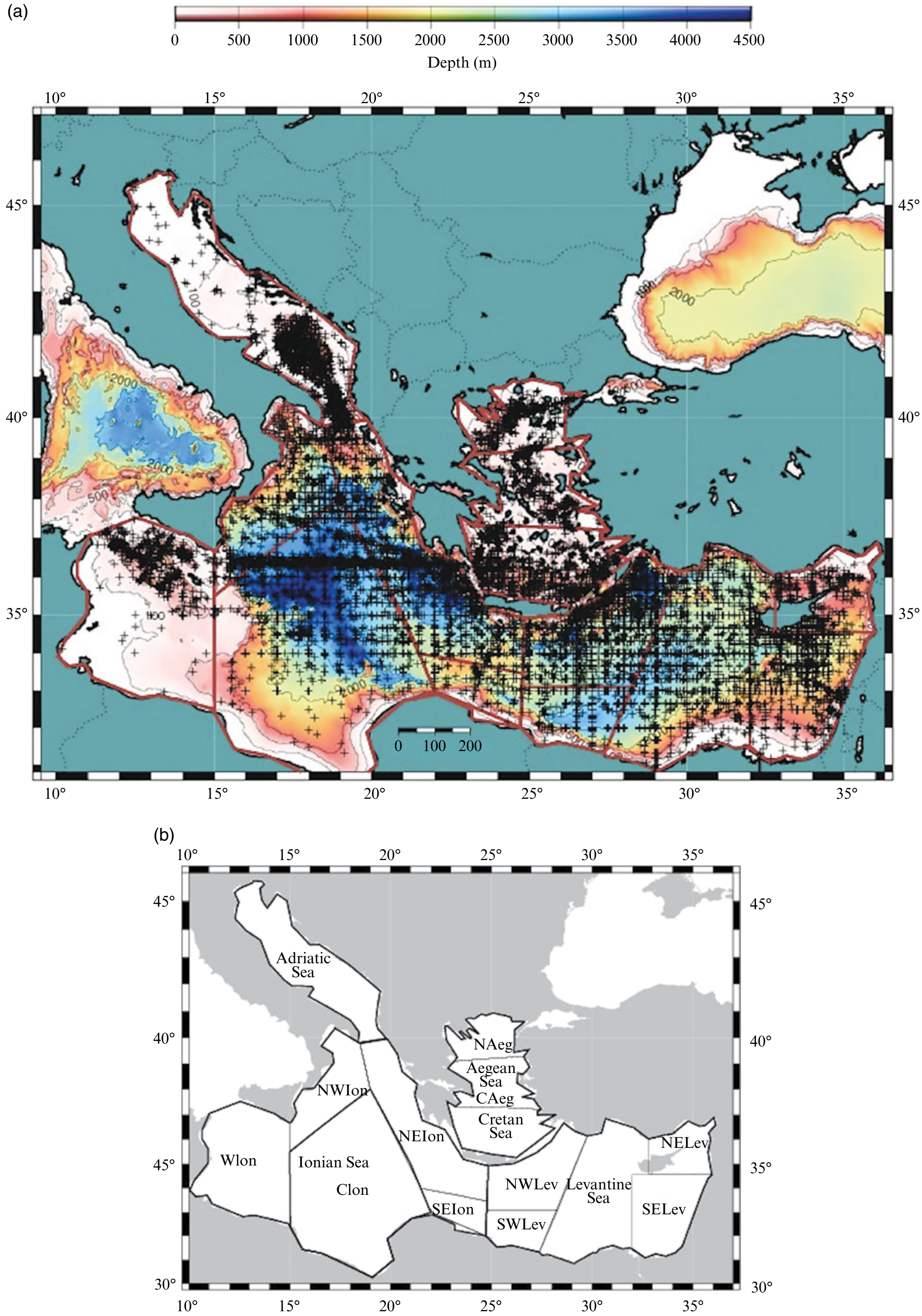

Figure 7.1. The Eastern Mediterranean Sea (a) bathymetry with overlaid station positions and subdomain boundaries, (b) subdomains of the study area. For color detail, please see color plate section.

the bin intervals were based on Student's t-test [*Emery and Thompson*, 2001], making use of the Numerical Recipes [*Press et al.*, 2007] library functions INVBETAI, BETAI, BETACF, and GAMMLN. The confidence interval, multiplying the standard deviation by a strong function of the number of samples, measures the reliability range of the estimated mean value, and therefore it is much reduced when there are a large number of observations proportional with the sample variance. The longer error bars in the plots appear when the number of observations or sample variance is smaller. In most cases, when there is a sufficiently large number of observations, the error bars are diminished and not clearly seen in the plots. However, we should also note that only a circular symbol for the data point without the error bar is displayed for the trivial case of a single observation in a bin, which is noted by not having a bar in the bar graphics showing the logarithm of the number of observations.

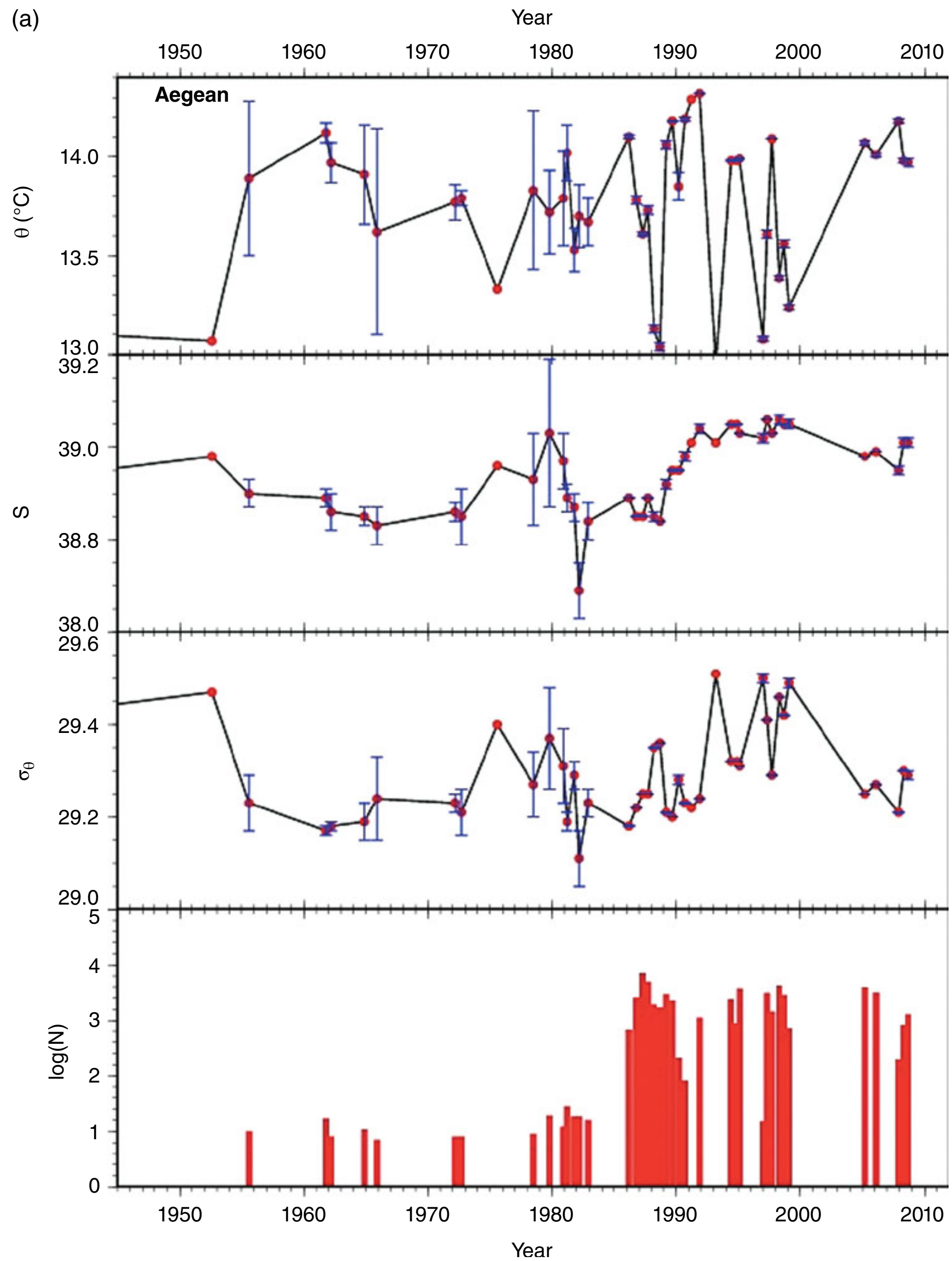

Figure 7.2. (a) Time series of average potential temperature, salinity, potential density, and log(N), the logarithm of the number of data points N in the 900–1100-m depth level, binned at half-year intervals in the Aegean Sea (vertical bars with end caps denote 95% confidence limits for data in each bin);

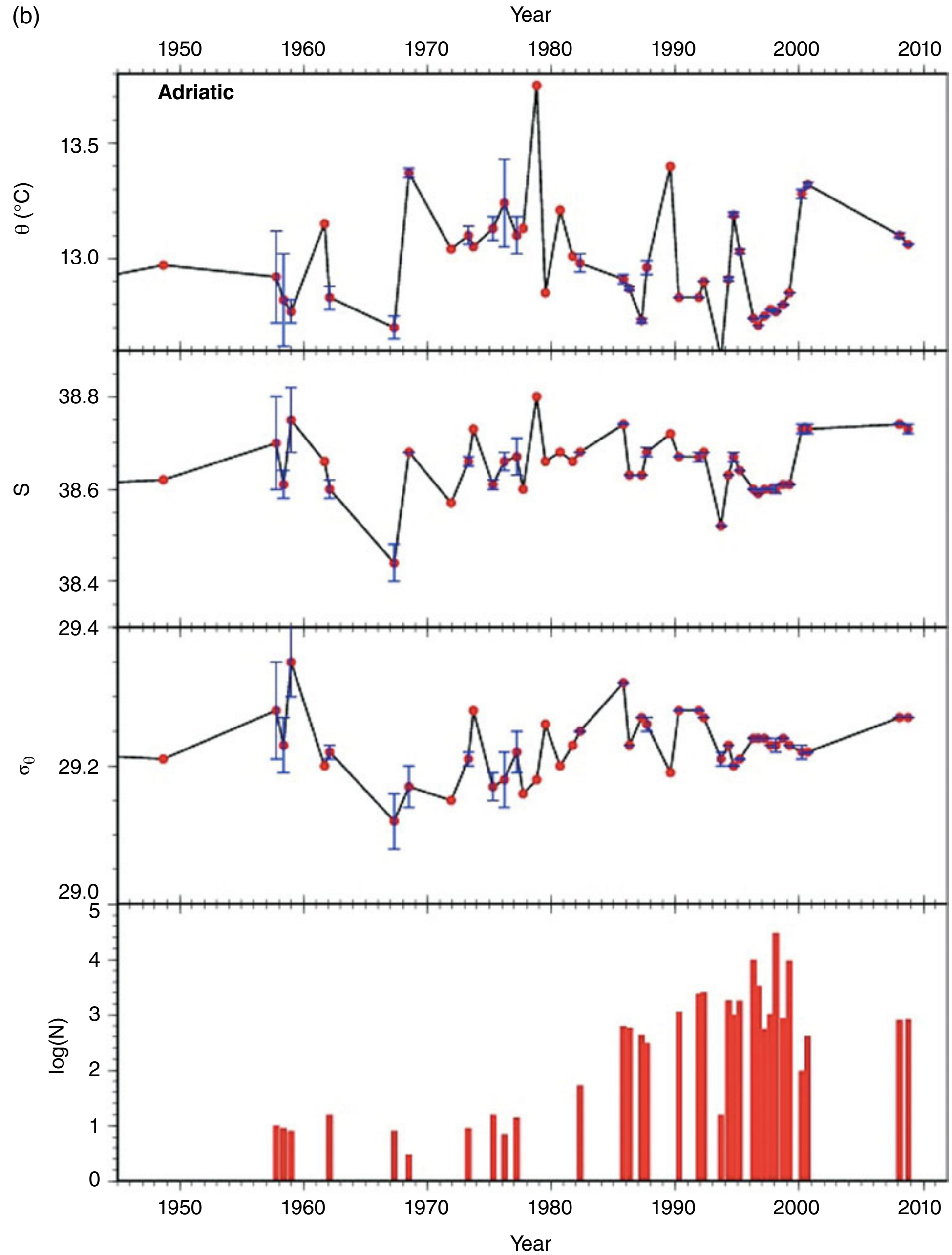

Figure 7.2. (continued) (b) time series of average potential temperature, salinity, potential density, and log(N), the logarithm of the number of data points N in the 900–1100-m depth level, binned at half-year intervals in the Adriatic Sea (vertical bars with end caps denote 95% confidence limits for data in each bin). For color detail, please see color plate section.

7.3. BASINWIDE AND INTERBASIN VARIABILITY

We first compare the general deep-water characteristics of the main subbasins of the eastern Mediterranean, namely, the Aegean and Adriatic shelf seas and the deep Levantine and Ionian basins, through a discussion of the water properties at the most relevant depth for each basin, 1 km for the Adriatic and the Aegean and 1–2 km for the Levantine and Ionian basins.

At depths centered at 1 km (Figure 7.2), the Aegean and the Adriatic seas have large oscillations of temperature, respectively with amplitudes of 1.5°C in the Aegean and 0.5°C in the Adriatic Seas. The cooling periods and patterns do not coincide in all cases. Recurrent decadal to multidecadal cooling periods with superposed shorter term events in 1950, 1970–1980, and 1990s are evident in both regions, with some mismatch between the two basins (see also Figures 7.6–7.9). In comparison, the Levantine and Ionian seas temperature centered at 1-km depth (not shown) displays much smaller interannual oscillations with amplitudes of 0.1–0.2°C. The higher amplitude response of the Aegean and Adriatic to surface effects is mostly related to the size of the basins, the associated sensitivity to atmospheric forcing, and the renewal timescales of the deep waters, which is much greater in the Levantine and Ionian seas.

In the Aegean Sea (Figure 7.2a), the most prominent feature in the time series is the steady rise of salinity continuing from the mid-1980s until the mid-1990s, which has been identified to be the result of a change in the Levantine circulation, the blocked circulation diverting saline water into the Aegean Sea [*Malanotte-Rizzoli et al.*, 1999]. The temperature is increasing along with salinity in the initial phase of this rise, but then the rapid cooling events in the early 1990s are ideal conditions for the massive formation of dense water in the Aegean Sea, as both the temperature and the salinity contribute to the abrupt density increase that has led to the EMT [*Özsoy and Latif*, 1996; *Theocharis et al.*, 1999].

On the other hand, at 2-km depth in the Levantine and Ionian basins (Figure 7.3), smaller oscillations of less than 0.1°C amplitude are detected until the early 1990s when abrupt, dramatic changes of more than 0.5°C in the Levantine and of 0.4°C in the Ionian basins occur in the form of interannual oscillations superposed on a stepwise change influencing the basin for the next two decades. The average temperature in the Levantine basin (Figure 7.3a), in fact, started to rise from 1988 onward, to reach a peak in 1993, followed by a secondary peak in 1997 and other oscillations in the following years.

The average temperature in the Ionian basin (Figure 7.3b) rose relatively more abruptly in 1992–1994, followed by a secondary peak in 1998–2001 in transient oscillations that seem to settle at about half the initial temperature rise. It appears that the outflow was felt immediately in both the Levantine and Ionian basins, but has led to greater changes in the Levantine Basin. Similar variations are detected in salinity, with an initial overshoot in 1993 that is larger than the stepwise change that follows. The overshoot signal in 1993 is present both in salinity and density, induced by the water sinking to these depths with the gravity current, although very little change persists in density in the later years, as the spreading of the anomalous waters appears to reach near equilibrium with the local density in the deep basin. We identify these changes to be tied to the cascading and spreading of the new dense water formed in the Aegean, verifying the long-term variations known as the Eastern Mediterranean Transient (EMT).

In addition to the temperature and salinity changes accompanying the EMT in the last two decades, there appear other significant peaks of salinity that influence the density in about 1980 in the Levantine Sea (Figure 7.3a), however without any significant changes in temperature. Similar small peaks of salinity without a signature in temperature occur in 1986 in the Ionian Sea (Figure 7.3b). These changes could be related to the intrusion of a water mass with salinity anomaly alone, or it is likely that some measurement errors could be involved in these cases.

Because salinity measurements have larger uncertainties and drifts due to instrumentation and sampling methods, we tend to rely more strictly on the temperature signals (see further discussion below), while evaluating salinity and density variations in parallel. In fact, in the case of the 1980 spike in the Levantine Sea (Figure 7.3a), the number of data points averaged is only about 10, reflected by the larger error bars (confidence intervals) in salinity and density in this period. In contrast, the 1993 salinity spike in the same figure provides much more confidence with several thousands of data points averaged, also coincident with the beginning signal of the EMT surviving later in the temperature anomaly. Other much smaller signals of simultaneous temperature and salinity variations affecting the density occur in the late 1960s and early 1970s both in the Levantine Sea and in the Ionian Sea.

In the deeper basins, the available temperature data centered at 3-km depth (Figure 7.4) shows a rapid rise of about 0.5°C in the Levantine Basin in 1992–1994, while a rise of about 0.2°C is indicated in the Ionian Basin in 1992–1995, followed by a secondary peak in 1998. Smaller peaks occur in the late 1960s and early 1970s in the Ionian Sea, but their significance is possibly limited, compared to the signals in the 1990s characterizing the EMT event influencing both deep basins of the eastern Mediterranean.

After the above description of clear signals in the deep temperature data, we turn our attention to the coevolution of water properties in the main basins. The potential temperature, salinity, and $\sigma\theta$ density at 0.5-, 1-, and 2-km depth layers, and the logarithm of the number of data points averaged for each bin at the respective depths in the Aegean Sea are displayed in Figure 7.5. For reasons of better visualization in a series of plots comparing properties at different depth intervals of each region, an offset factor proportional to n (where n = 0, 1, 2, 3, corresponds to the number assigned to each depth interval) is subtracted from the parameters' values. In the bottom panel of each plot, the number of data points entering the half-year time bins is shown in logarithmic scale (e.g., log(N) = 3 corresponds to data averaged from 1000 measurement points).

Temperature in the Aegean Sea, at the first two levels of Figure 7.5, shows interannual and decadal oscillations resulting in cooling by about 1.5°C for each of the events in the 1987–1989, 1993, 1997–1999 periods, while the third level at 2-km depth is relatively constant with a higher value between 1986–1994. This is almost the same period when salinity is on the rise at all displayed depth levels, that is, the period of saline water entry into the Aegean Sea noted in the literature [*Theocharis et al.*, 1999; *Malanotte-Rizzoli et al.*, 1999]. We should note, however, that the sawtooth pattern in temperature of the first two depth levels after the 1990s is a result of the uneven distribution of data in the whole of the Aegean Sea, with the colder observation points located in the northern and central Aegean subdomains (compare with Figure 7.10).

The uniform increase of salinity at all deep layers of the Aegean Sea during the 1985–1995 period is very interesting. If the increase were to be attributed to the LIW import from the Levantine Sea alone, it would be hard for the rather shallow LIW to influence the deeper layers. This observation, that needs further investigation, implies that deep-water formation processes in the

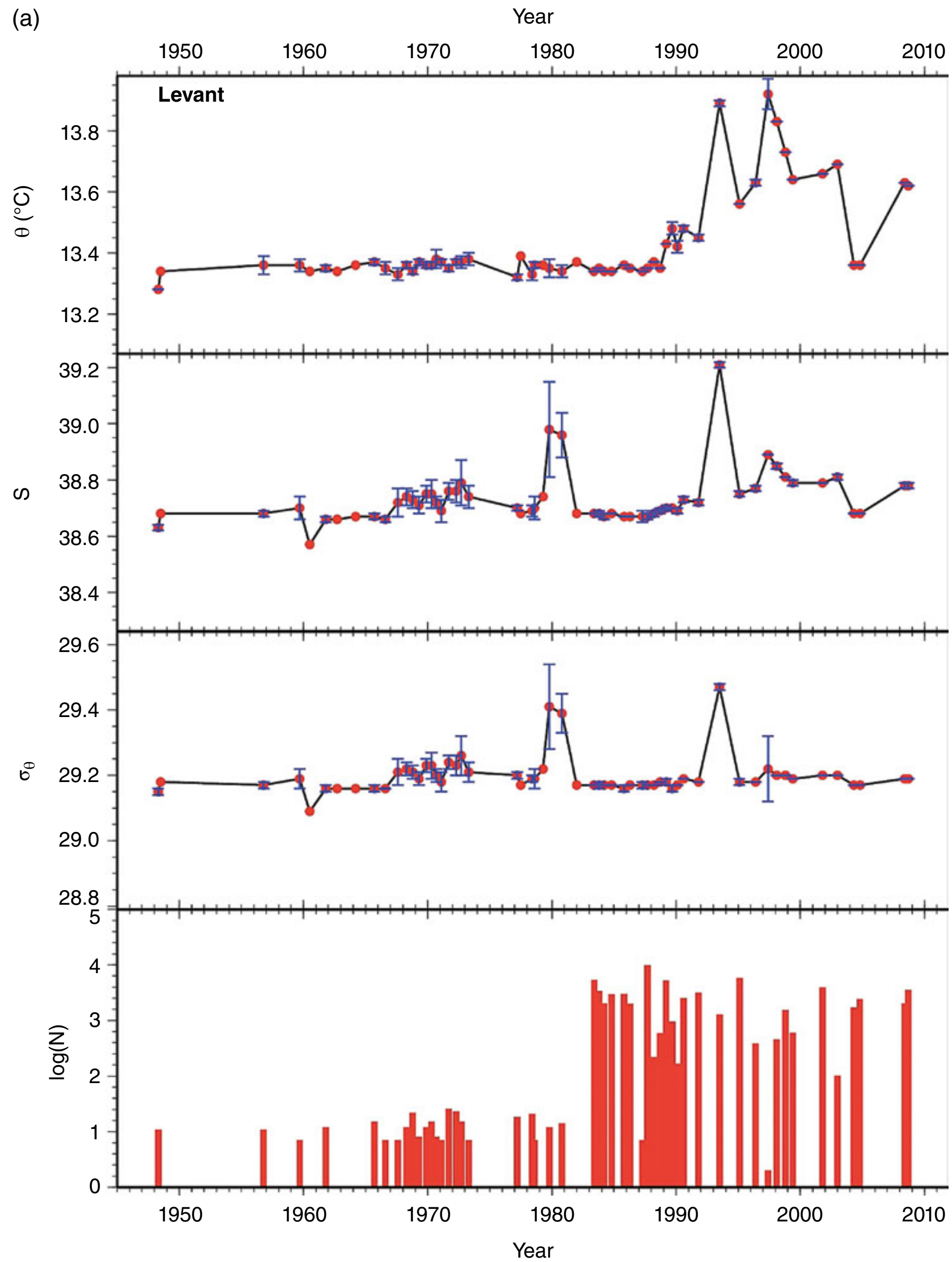

Figure 7.3. (a) Time series of average potential temperature, salinity, potential density, and log(N), the logarithm of the number of data points N, in the 900–1100-m depth level, binned at half-year intervals in the Levantine Sea (vertical bars with end caps denote 95% confidence limits for data in each bin);

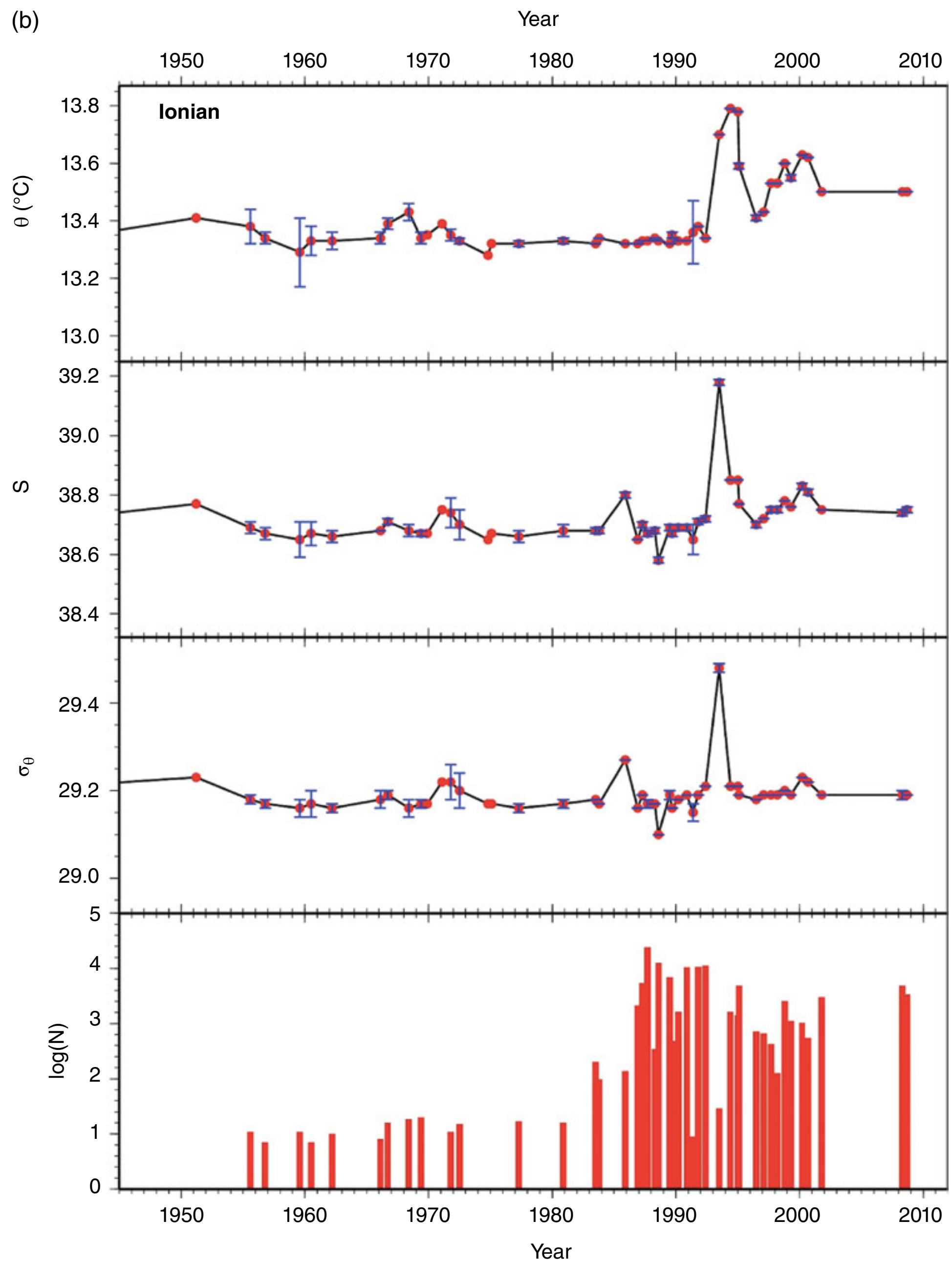

Figure 7.3. (continued) (b) time series of average potential temperature, salinity, potential density, and log(N), the logarithm of the number of data points N in the 900–1100-m depth level, binned at half-year intervals in the Ionian Sea (vertical bars with end caps denote 95% confidence limits for data in each bin). For color detail, please see color plate section.

Aegean Sea were affecting the whole water column. The salinity at the first two levels has marked interannual to decadal oscillations before and after this period, but the last level of 2-km depth reaches almost an asymptotic value after a salinity rise of about 0.2 in the period 1985–1995. The density increase to peak values in the late 1990s is recovered in later years at the first two levels but not in the deepest layer. The waters in the deeper parts of the basin (that are isolated by abrupt topography) are not yet affected by the post-EMT temperature and salinity variations in the shallower parts of the basin. This was also recorded in two cruises (2005–2006) with observations at the deepest parts of the Aegean Sea [*Vervatis et al.*, 2011].

The Adriatic Sea in Figure 7.6 displays interannual to decadal oscillations, but much smaller than those

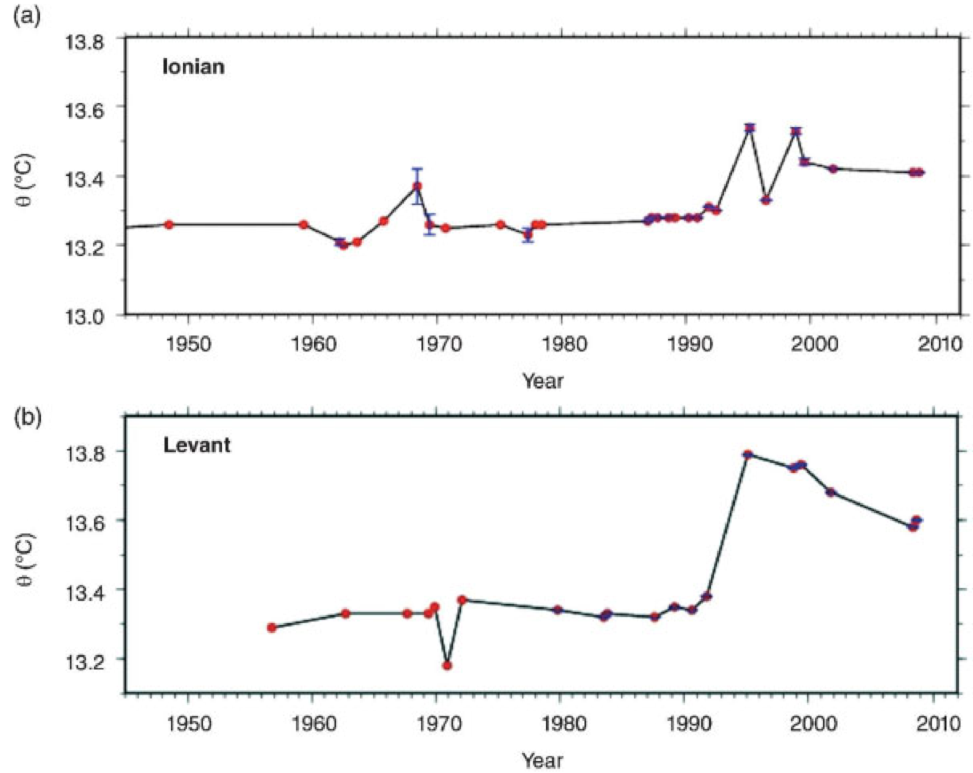

Figure 7.4. Time series of average temperature at depths of 2900–3100 m binned at half-year intervals in the (a) Ionian and (b) Levantine Seas. For color detail, please see color plate section.

observed in the Aegean Sea. A stepwise rise of salinity or density resembling the one in the Aegean Sea is not discernible during the observation period. If any dense-water production event should be responsible for an Adriatic contribution to the EMDW, it would have to be linked to these oscillations. We note temperature and salinity decreases in the 1960s, in 1987, and in the 1989–1994 periods, especially in the 0.5-km depth layer. The latter period of 1987–1994 coincides with the EMT period, and overlaps with the 1988–1997 period of anticyclonic circulation in the Ionian Sea, when a decrease has been observed in the Adriatic salinity [*Gačić et al.*, 2010]. On the other hand, temperature and salinity increases are found in the 1973–1983 and 1998–2001 periods, partially overlapping with the 1998–2006 period of cyclonic circulation in the Ionian Sea when an increase is observed in the Adriatic salinity [*Gačić et al.*, 2010]. The density in the 1.0-km layer appears to increase in the 1970s, early 1980s, and early 1990s periods.

Because the EMT appears dominating in the time history of the deep Levantine and Ionian seas properties, we focus our attention on the immediate neighborhood of the Cretan Sea source, *that is*, the northwestern Levantine and the northeastern Ionian seas regions where most of the variability is encountered, rather than providing basinwide changes in this section. The basinwide changes in properties at 2-km depth have already been reviewed in Figure 7.3.

In the northwestern Levantine Sea (Figure 7.7), a cooling event is detected at the first level of 0.5-km depth in the years 1993–1994, coinciding with other changes in the deeper layers in the ensuing EMT period. Stacked plots of properties indicate stepwise increases of temperature and salinity at depths centered at 2- and 3-km depths in the early 1990s following the EMT. Salinity spikes at the depth layers 0.5, 1, and 2 km are coincident with beginning of EMT anomalies at the same depths, while only a stepwise increase of salinity is detected in the 3-km depth layer. This is because the introduction of the new water masses into the Levantine basin during the EMT event occurs in the form of a deep overflow from the Aegean straits, which then spreads in the entire Levantine Basin and continues to influence the basin throughout the next two decades.

It is also interesting that there is no discernible net increase in density after the EMT event except the transient anomalies and the slight increase in the 3-km depth layer, suggesting that the overflow from the Aegean Straits largely interleaves into the existing stratification without actually changing the density significantly, because of the compensating nature of the warm temperature against the higher salinity of the outflow. *Roether*

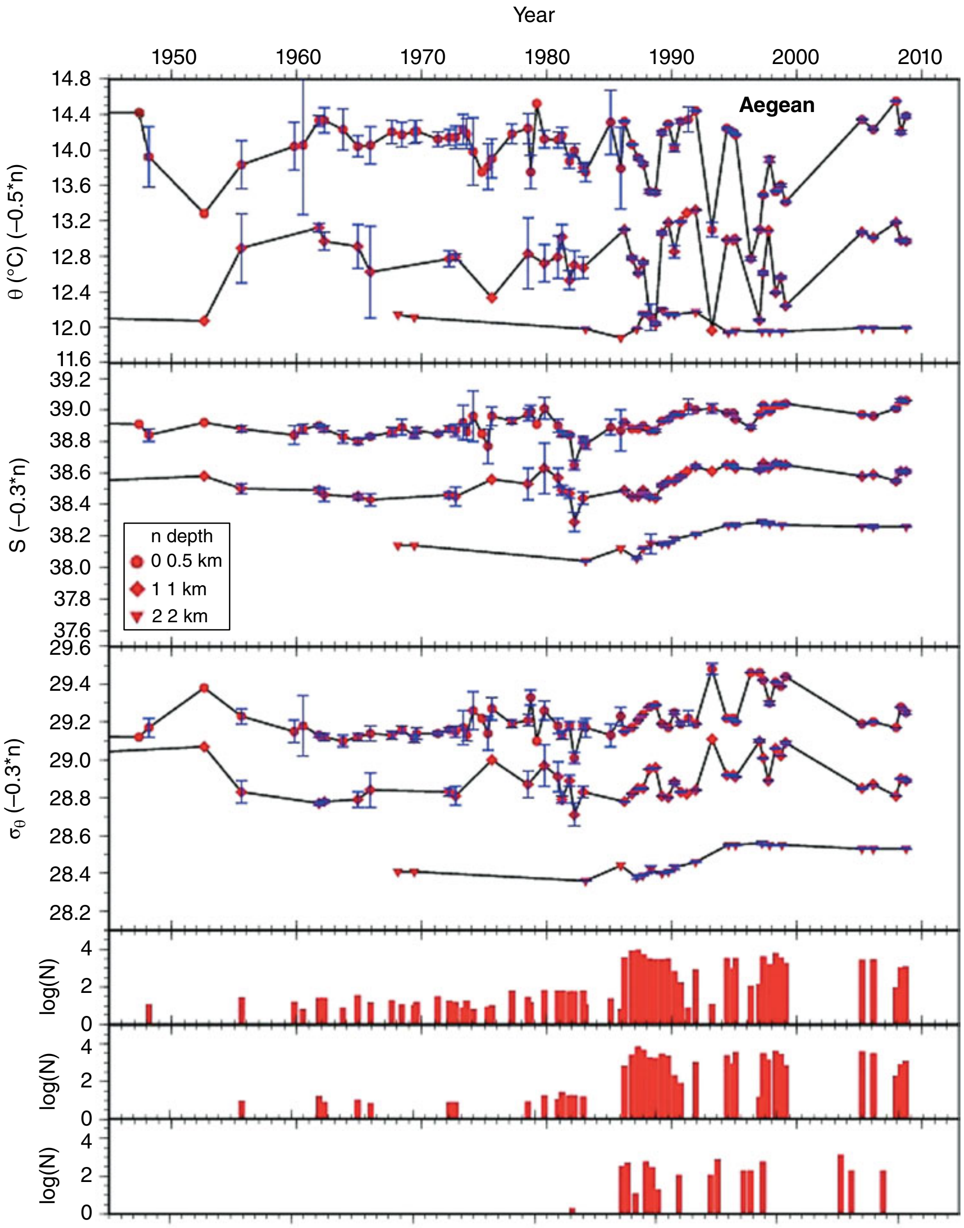

Figure 7.5. Aegean Sea potential temperature θ, salinity, and σ_θ density at depth layers of 450–550 m (n = 0), 900–1100 m (n = 1), and 1900–2100 m (n = 2) (vertically shifted down by a constant times n) and log(N), the logarithm of the number of data points N averaged for each half-year bin interval. (Vertical bars with end caps denote 95% confidence limits for data in each bin.) For color detail, please see color plate section.

et al. [2007] have argued that the dominance of the Aegean source was primarily a result of rates and much less of density. They find that after 1994, the near bottom flow was driven by extremely low lateral density gradients that were also nearly invariant in time.

While the EMT associated temperature increase in the deepest layers seems to have occurred only after the 1990s, and an absolutely stable temperature record is found before this period without a notable trace of change up until the late 1980s, the same cannot be said for salinity and density. It seems that short periods of increased salinity occurred around 1960, 1970, and the 1980s, but without a trace in temperature, which means that peaks in density follow the influence of salinity. The salinity peaks producing effects on density without a compensating temperature change in around 1980 have higher error bars based on few stations available, as discussed earlier in relation to Figure 7.3.

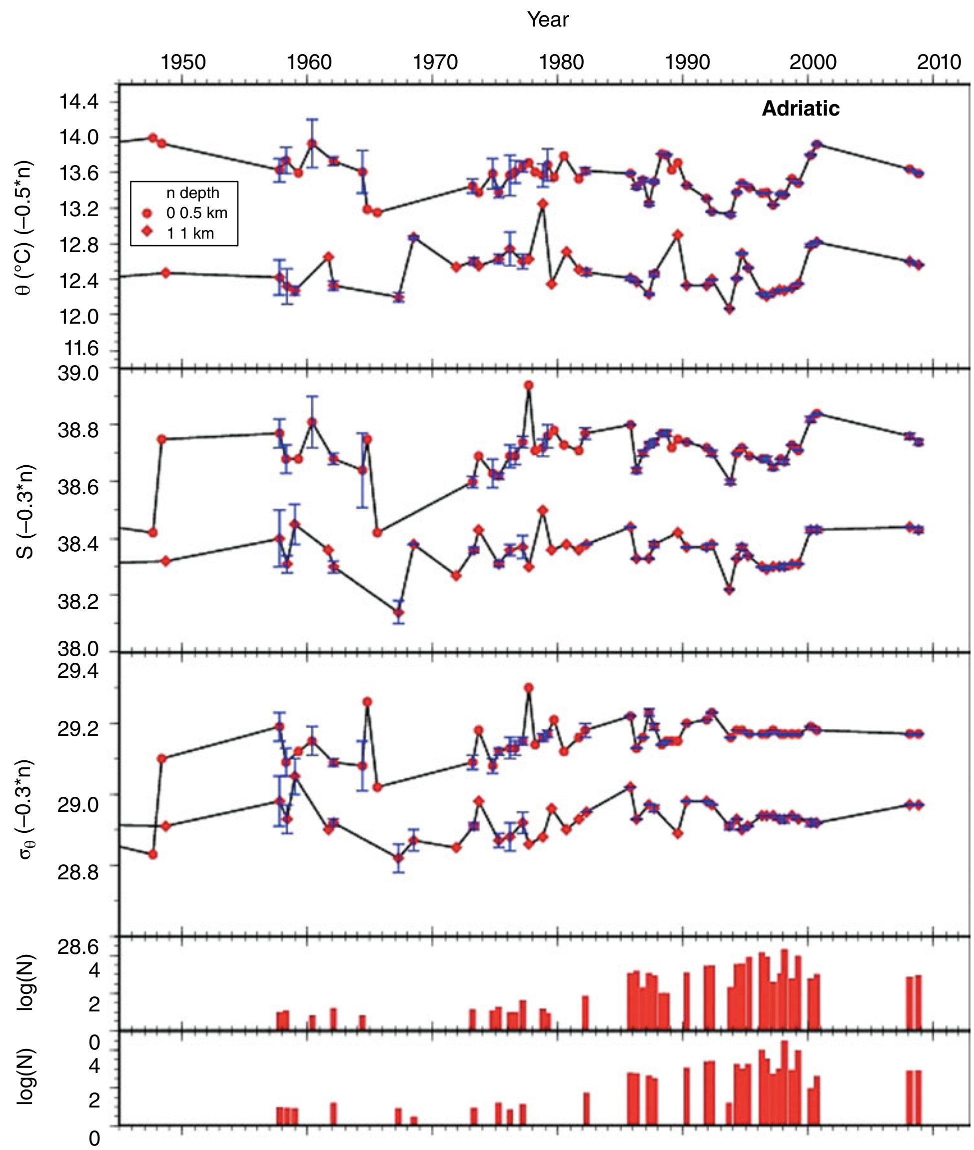

Figure 7.6. Adriatic Sea potential temperature θ, salinity, and σ_θ density at depth layers of 450–550 m (n = 0) and 900–1100 m (n = 1) (vertically shifted down by a constant times n), and log(N), the logarithm of the number of data points N averaged for each half-year bin interval. For color detail, please see color plate section.

We next present results for the northeastern Ionian Sea (Figure 7.8), where salinity peaks occur at all displayed depth levels, coinciding with the largest signal in temperature at the 2- and 3-km depth levels, marking the outflow of dense water from the Aegean into the Ionian Sea during the EMT. The first level at 0.5-km depth interval shows a continuous cooling trend from the 1980s onward, until a stronger cooling event is observed in the first half of the 1990s, coinciding with a peak in salinity at this and lower layers.

The positive temperature and salinity anomalies observed at the deep layers during the EMT events in some time-series plots may appear unnatural when cooling is expected from an event of convective origin. However, this is related to the production of a new deep-water mass during the EMT, when waters of greater salinity in the Aegean Sea did not have to undergo very extensive cooling in order to reach very large densities and sink and spread in almost all the eastern Mediterranean Sea. Turbulent entrainment processes also influence the final characteristics of the spreading water mass, as indicated by the higher salinity and temperature of the anomalous waters arriving at the deeper levels. The positive anomalies observed at depths greater than 0.5 km in the Levantine and Ionian seas illustrate the fact that the source of water is external to these basins, as it clearly originates from the neighboring Aegean Sea.

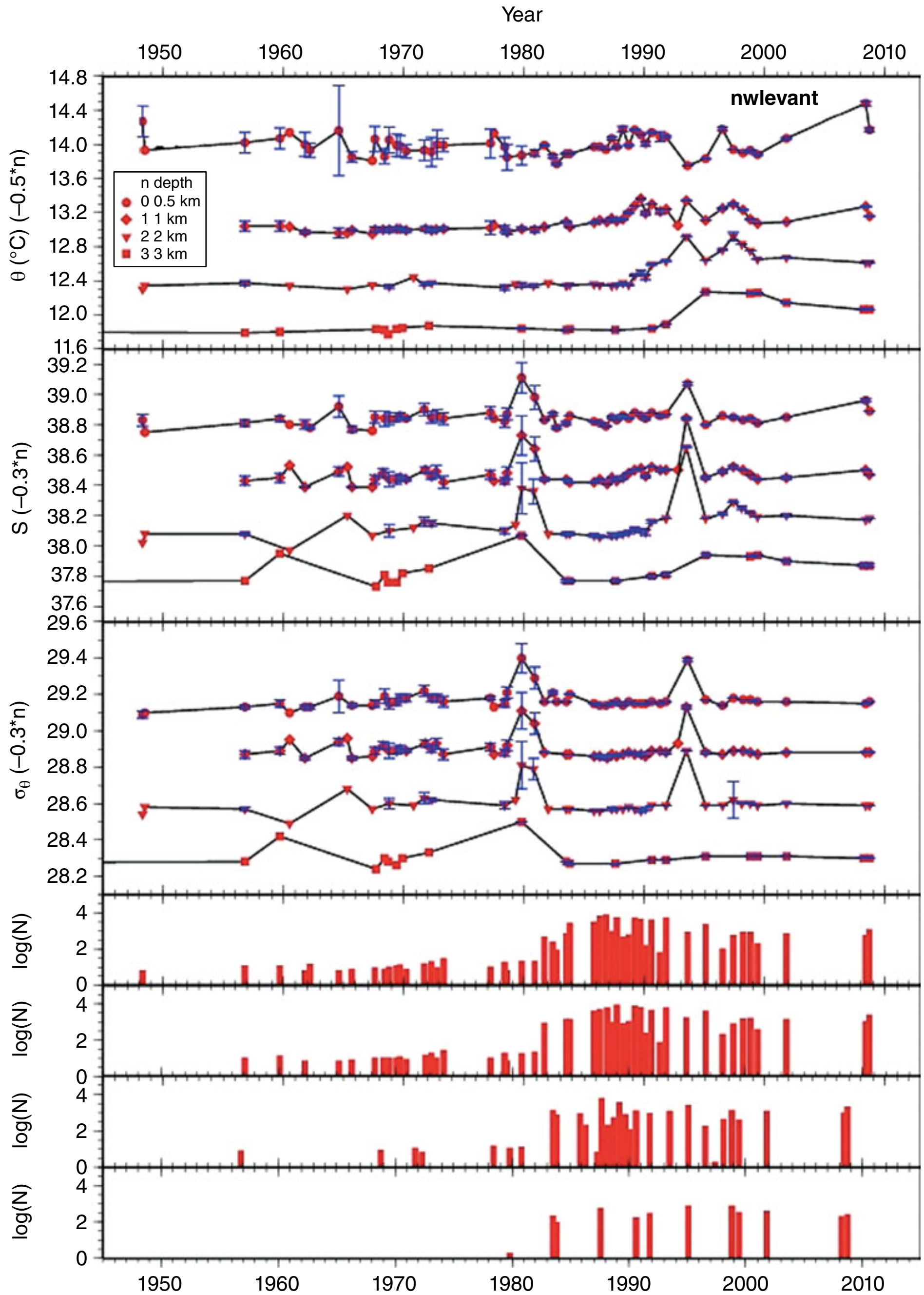

Figure 7.7. Northwestern Levantine Sea potential temperature θ, salinity, and σ_θ density at depth layers of 450–550 m (n = 0), 900–1100 m (n = 1), 1900–2100 m (n = 2), and 2900–3100 m (n = 3) (vertically shifted down by a constant times n) and log(N), the logarithm of the number of data points N averaged for each half-year bin interval. For color detail, please see color plate section.

In Figure 7.9 we provide the density variations at 4-km depth in the deepest troughs of the Levantine and Ionian seas, respectively in the northwestern Levantine and central Ionian subdomains. A decrease in bottom layer density is detected in the northwestern Levantine (Rhodes) depression after the EMT period, while an increase is detected in the central Ionian depression, the density being equalized at a value of about 29.2 in both basins after the 1990s. We should note, however, that the number of observations prior to the 1990s is limited to a single one for each time bin, while it is increased to about 100 profiles per bin in the latter period, increasing the reliability of the observations in the last two decades.

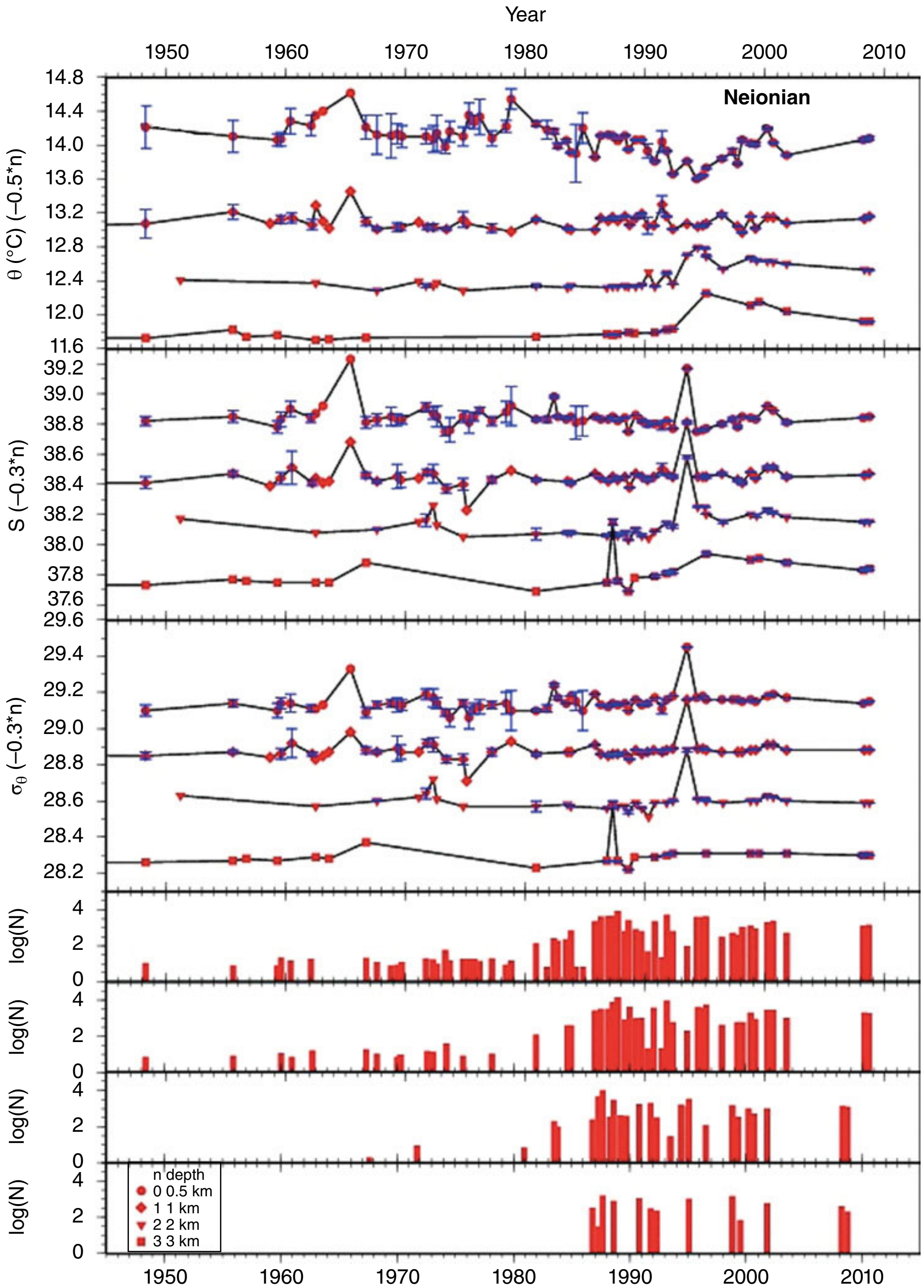

Figure 7.8. Northeastern Ionian Sea potential temperature θ, salinity, and σθ density at depth layers of 450–550 m (n = 0), 900–1100 m (n = 1), 1900–2100 m (n = 2), and 2900–3100 m (n = 3) (vertically shifted down by a constant times n), and log(N), the logarithm of the number of data points N averaged for each half-year bin interval. For color detail, please see color plate section.

7.4. INTRABASIN VARIABILITY

We next review the behavior of the subdomains within the Aegean Sea in Figure 7.10. The Aegean Sea played a key role in the largest event of deep-water variability in the eastern Mediterranean Sea. Furthermore, its geography and topography is the most complicated in the region, with thousands of islands and islets and a large number of depressions and sills. The Aegean Sea is mainly a shelf sea, with most of the basin having shallow depths except the three deep basins of the north Aegean (the North Aegean trough consisting of the Sporades, Athos, and Lemnos basins), the central Aegean (Skiros and Chios basins), and the southern Aegean Sea (Cretan Basin).

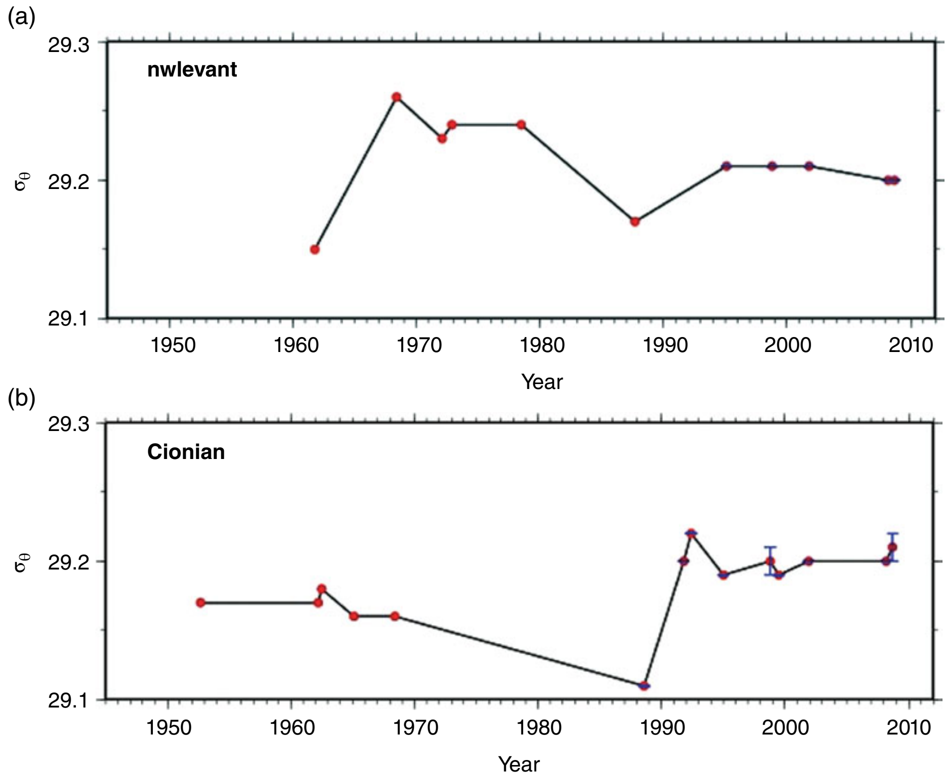

Figure 7.9. Potential density in the 3900–4100-m depth interval in the (a) northwestern Levantine and (b) central Ionian subdomains representing the deepest areas of the Levantine and Ionian seas. For color detail, please see color plate section.

In the north Aegean Sea (Figure 7.10a) at depth layers centered at 0.5- and 1-km depth, a very strong cooling event occurs in the late 1980s followed by a steady increase in salinity, leading to the highest densities in the late 1990s. In fact, the mean potential density values of up to 29.53, reached in the bottom waters of the north Aegean Sea in the mid-1990s, are the highest values observed anywhere in the entire Mediterranean Sea.

A rather stronger cooling event occurred at the earlier period of 1987–1989 in the northern and central basins [*Gertman et al.*, 2006], but it is absent in the Cretan Sea, which together with the increasing trend of salinity in the entire Aegean Sea, may have served in the preconditioning of properties. In the north Aegean (Figure 7.10a), data are insufficient to show a strong cooling event in the years 1992–1993, but there are enough data to show this in the central Aegean basin (Figure 7.10b).

A stagnant period in the years 1994–2000 followed the density maximum in the mid-1990s and survived till many years later [*Zervakis et al.*, 2003; *Androulidakis et al.*, 2012], as a result of the increased stability and the combined influences on surface buoyancy created by the net water fluxes at the sea surface and the changes in the flux of Black Sea Water (BSW) outflowing from the Dardanelles Strait.

In the Cretan basin layers of 1 and 2 km (Figure 7.10c), interdecadal oscillations of 10–15-year periods are observed both in temperature and in salinity and density. These oscillations reach a plateau after the early 1990s EMT event, following a period of steady increase in salinity in the 1980s and the cooling event in 1992–1993. The high-density deep waters filling the deeper part of the Cretan Basin seem to have reached a rather stable situation after the 1990s, at least until the present. According to *Theocharis et al.* [1999], the deep basin of the Cretan Sea had been filled by dense Cretan Deep Water (CDW) starting in 1987 and lasting until 1992–1993, when the first dense-water outflow from the Cretan Strait was initiated. Continued observations reported by *Theocharis et al.* [2002] seemed to indicate a return to pre-EMT conditions after the mid-1990s, with continued but smaller overflows contributing only to the midlevels of 1.5–2-km depth in the exterior region.

Our analysis in Figure 7.10c shows that the increase in salinity started after the strong cooling period in the early 1980s and lasted until mid-1990s. The salinity and density in the deeper basin at 2 km stayed stationary, but decreased slightly after the mid-1990s maxima. Further review of Figures 7.11 and 7.13 will emphasize the fact that a net stepwise rise in the temperature signal has been preserved at both 1- and 2-km depth until the last decade, although large fluctuations are superposed on this rise.

On the other hand, stronger cooling events seem to have taken place during the 1970s and 1980s, but in these cases the cooling periods were also associated with lower salinity, and therefore without any increase in the density. The difference in the early 1990s case was that an increase in salinity occurred throughout the entire later part of the 1980s until 1991 (preconditioning phase), and with the cooling imposed on this situation it probably created sufficiently high density to initiate the outflow from the Cretan Sea into the adjacent seas.

It may also be observed in Figure 7.10 that the density is always higher in the northern basin of the Aegean as compared to the central and southern basins, but in the case of the 1990s EMT period, density in the deeper northern and central basins approach each other almost to be equalized, though remaining much higher than the

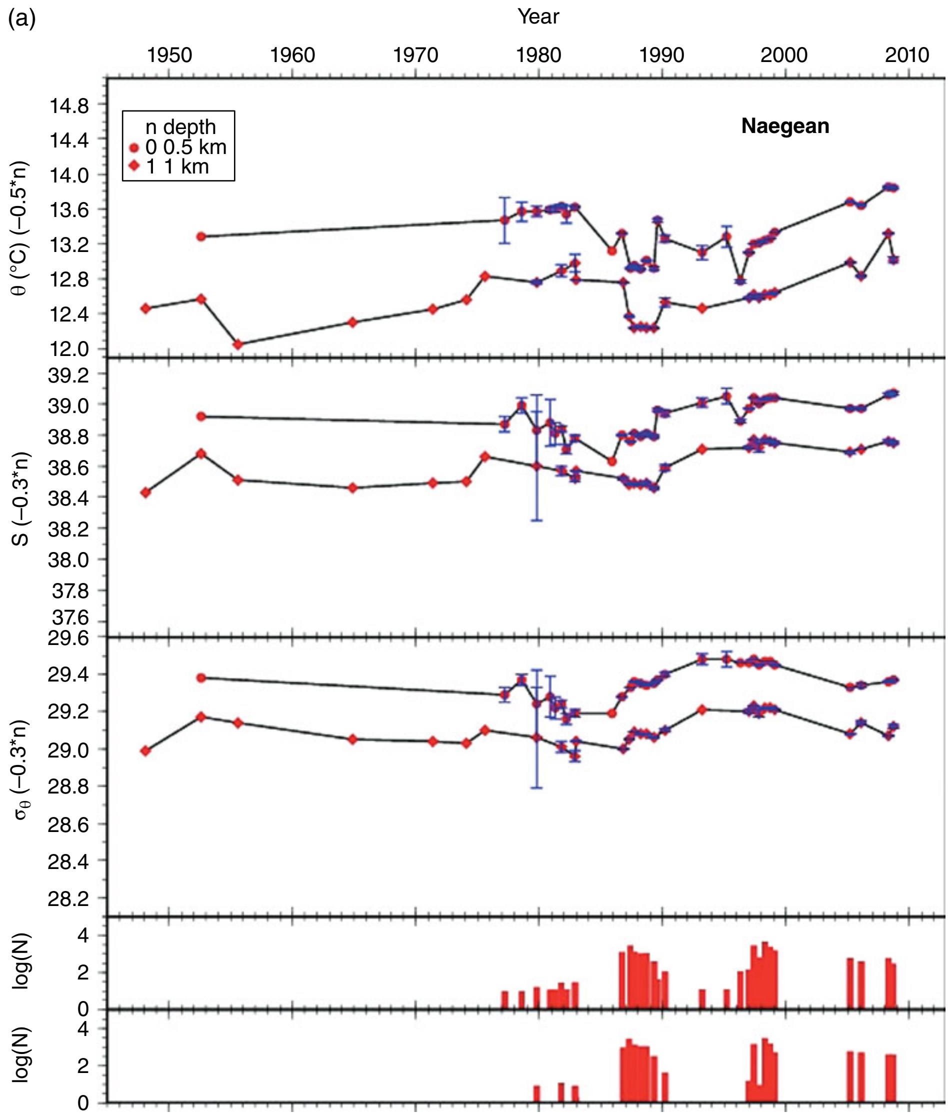

Figure 7.10. (a) North Aegean Sea potential temperature θ, salinity, and σ_θ density at depth layers of 450–550 m (n = 0), 900–1100 m (n = 1), and 1900–2100 m (n = 2) (vertically shifted down by a constant times n) and log(N), the logarithm of the number of data points N averaged for each half-year bin interval; (b) Central Aegean Sea potential temperature θ, salinity, and σ_θ density at depth layers of 450–550 m (n = 0), 900–1100 m (n = 1), and 1900–2100 m (n = 2) (vertically shifted down by a constant times n) and log(N), the logarithm of the number of data points N averaged for each half-year bin interval; (c) Southern Aegean Sea (Cretan Sea) potential temperature θ, salinity, and σ_θ density at depth layers of 450–550 m (n = 0), 900–1100 m (n = 1), and 1900–2100 m (n = 2) (vertically shifted down by a constant times n), and log(N), the logarithm of the number of data points N averaged for each half-year bin interval. For color detail, please see color plate section.

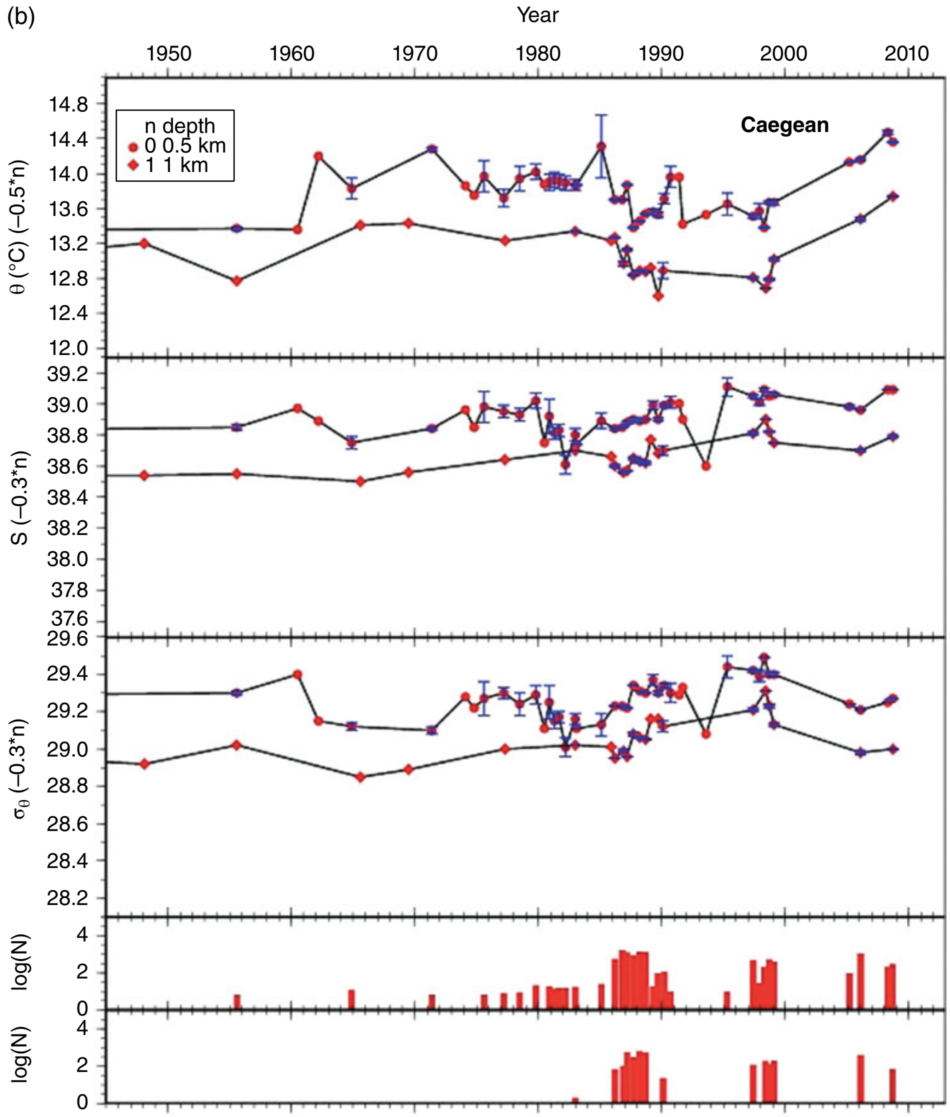

Figure 7.10. (continued)

density at the same depths in the Cretan Sea. It is also discernible in Figure 7.10 that the stratification in the Cretan basin increases in parallel with the period of steep increases in salinity and density during the 1983–1993 period. The same can be said for the central Aegean basin only in the 1980–1990 period, though the stratification appears weaker during the rest of the observed period.

Sayın and Beşiktepe [2010] confirm some of these results based on measurements made in the north Aegean on the eastern side of the north Aegean trough (Saros deep and Limnos north), north of the central Aegean (Limnos south), and on the eastern side of the Cretan Sea (south Aegean). Through analyses of these partial data, they have shown the mixing to a depth of 200 m producing water of density greater than 29.5 south of Limnos Island in the central Aegean region, but they have missed completely the same levels of density reached in the north Aegean. *Sayın and Beşiktepe* [2010] also note the cyclonic circulation of the central Aegean aiding northerly transport of saline water on the eastern flank and the transport of dense water south by the same circulation. This could be an additional factor for transporting dense water to the Cretan Sea while withdrawing more saline water from the south, eventually contributing to the dense-water formation in the north.

The role of the Central Aegean Sea in the regional thermohaline circulation and deep-water formation was also investigated during the 2005–2006 cruises [*Vervatis et al.*, 2011]. They recorded dense-water formation processes and found that the central part of the basin plays a very important role for the whole basin. Due to the presence of high salinity waters of Levantine origin,

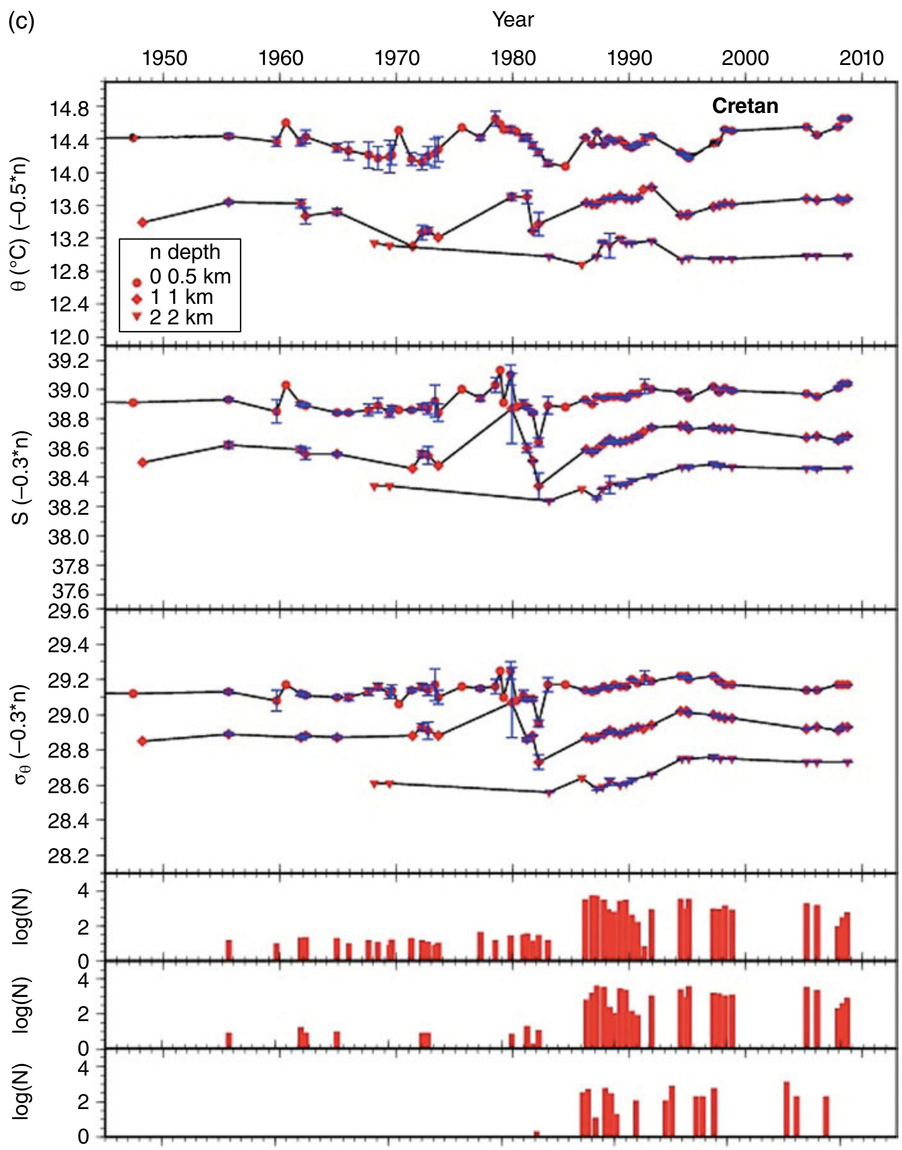

Figure 7.10. (continued)

the strong atmospheric forcing and its shape, it is the most prominent area for dense-water formation and can act as a reservoir of dense waters for the adjacent Aegean subbasins. This contribution of the central Aegean Sea to the intermediate and deep layers of the Aegean Sea, also identified by two cruises in the late 1980s and early 1990s [*Gertman et al.*, 2006], can also explain the larger salinity increase signal in the central and northern parts of the Aegean Basin and the amplified signal in the deeper levels of the Cretan Sea.

We believe the salinity increase that led to the density increase in the deep Northern Aegean Trough resulted from the LIW entering into the Aegean Basin and penetrating to the central and north Aegean during this period, as a result of the blocked circulation in the Levantine Sea as observed in October 1991 [*Theocharis et al.*, 1999; *Malanotte-Rizzoli et al.*, 1999]. Contributions of increased E-P [*Josey et al.*, 2011] and reduced BSW inflow in the Aegean Sea [*Zervakis et al.*, 2000] were also proposed as mechanisms for the density increase observed in the basin. Once the wheel starts to turn, that is, when the outflow of dense water out of the Aegean starts, there would be more saline water entering in replacement as *Sayın and Beşiktepe* [2010] proposed. However in Figure 7.9, we see that the increase in salinity starts much earlier in the late 1980s, possibly after the extensive cooling in the north Aegean, which may have initiated at least one of the triggers.

The analysis of spatial variations across the deep Levantine and Ionian basins is carried out on the basis of

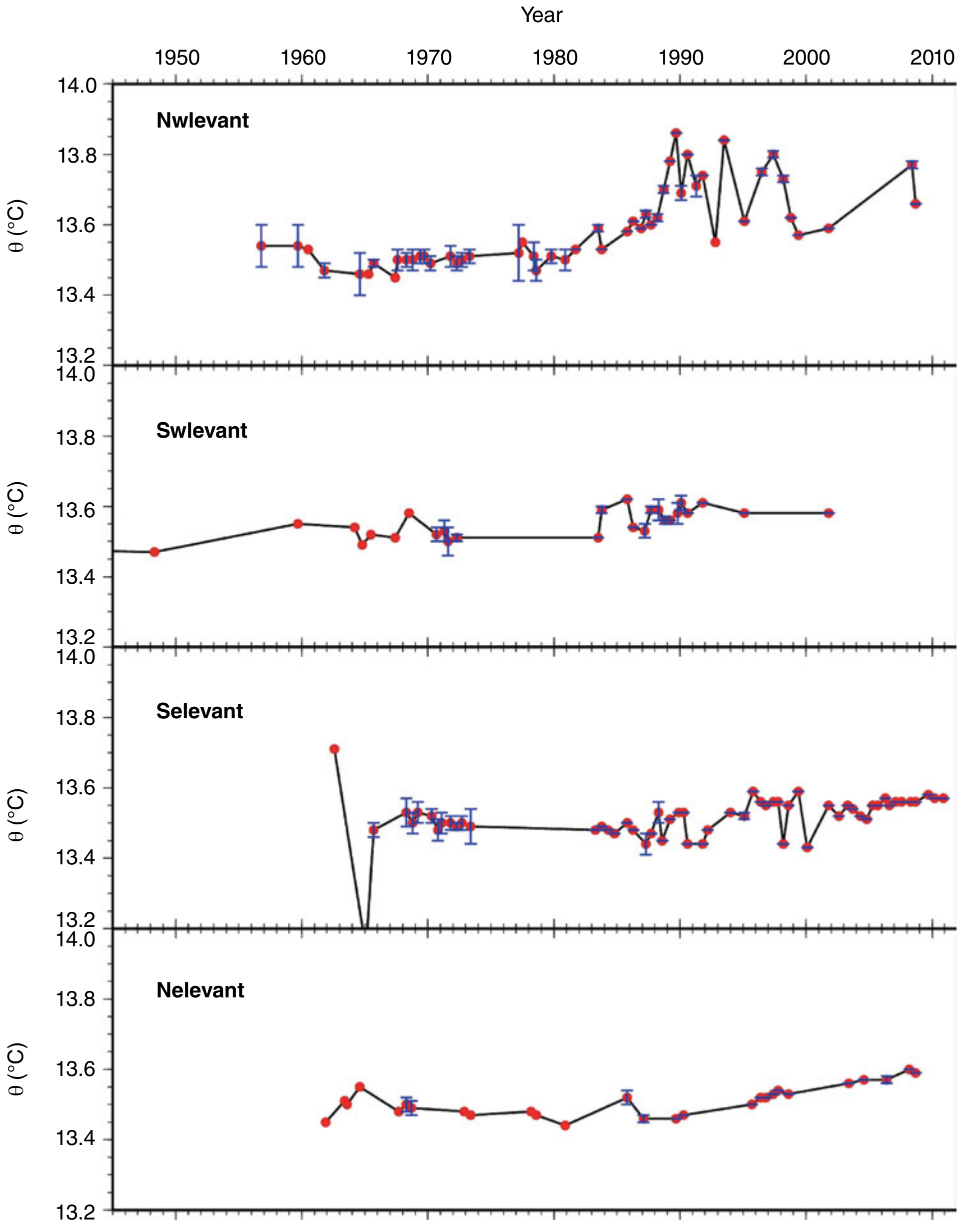

Figure 7.11. Potential temperature θ in the 900–1100-m depth level in the (a) northwestern, (b) southwestern, c) southeastern, and d) northeastern Levantine subdomains. For color detail, please see color plate section.

temperature data, built upon the confidence we have on the measurement of temperature. Although salinity is usually considered as a conservative tracer in the ocean, in this case we prefer to use temperature as a more reliable tracer for better detection of deep-water changes. We trace these changes based on the comparison of time-series between subdomains of the Levantine and Ionian seas at the 1- and 2-km depth levels in Figures 7.11–7.14, respectively.

The distinct pattern of the temperature time-series at 1-km depth in the northwestern Levantine region (Figure 7.11a) is clearly differentiated from the other time-series in the various Levantine Basin subdomains at the same depth (Figure 7.11). In this region, the temperature starts rising continuously from the early 1980s onward, reaching a peak in 1989 and oscillating afterward, with other peaks in 1992, 1997, and 2008, by a total temperature rise of about 0.4°C. Combined with the interpretation of Figure 7.7 showing parallel changes in temperature and salinity at all depths, the enlarged plot in Figure 7.11a shows that the preconditioning evolution that leads to the EMT starts in the second half of the 1980s, much earlier than 1992. It can also be understood that the overflow of anomalous waters from the Cretan

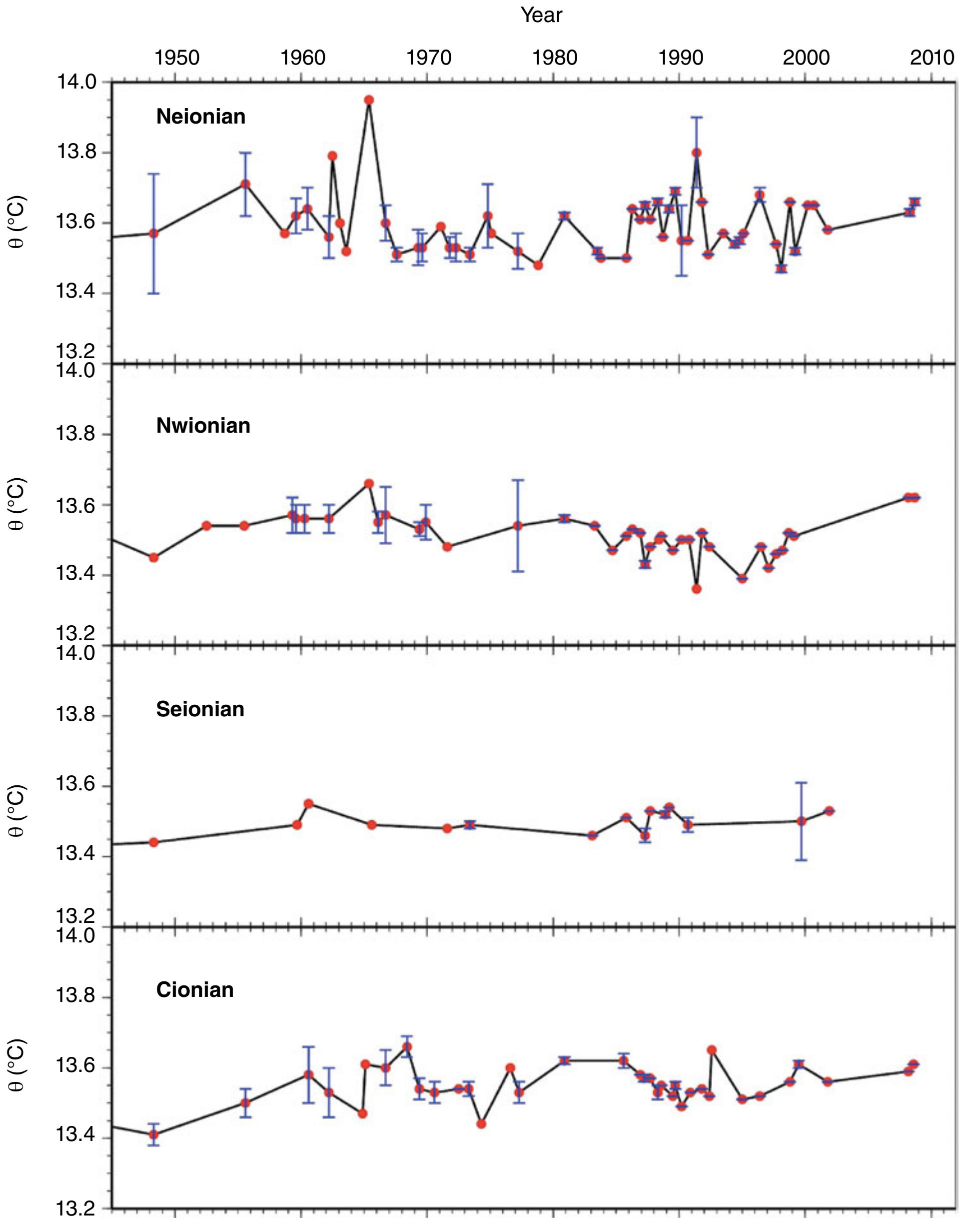

Figure 7.12. Potential temperature θ in the 900–1100-m depth level in the (a) northeastern, (b) northwestern, (c) southeastern, and (d) central Ionian subdomains. For color detail, please see color plate section.

Sea has started much earlier than the peak of the EMT signal in 1992–1993.

Barely noticable increases of 0.1–0.2°C are indicated in the southwest and southeast regions (Figures 7.11b,c) almost synchronous with the northwest after the 1980s, but not followed by the later sequence of peaks and the clear stepwise increase observed there. The northeast box indicates only a continuous trend of increasing temperature during the same period (Figure 7.11d). The Ionian Basin northeast, northwest, southeast, and central subdomains (Figure 7.12a–d) all have different patterns of similar magnitude, none of them indicating a pattern that comes close to the signature in the nortwestern Levantine box from starting in the second half of the 1980s.

The above discussion shows that the largest anomalies occur only in the northwest Levantine area in the 1-km depth level, reflecting the influence of the new dense water from the Cretan Sea into the Levantine Sea in its neighborhood. Studies carried out in the pre-EMT and post-EMT periods show that the stratification of the Aegean Sea and its adjacent basins are influenced by the exchange fluxes in the Cretan Arc straits system [*Zodiatis*, 1992, 1993; *Kontoyiannis et al.*, 2005]. It is probably through the Kasos Strait, with a sill depth of 1000 m at its deepest point east

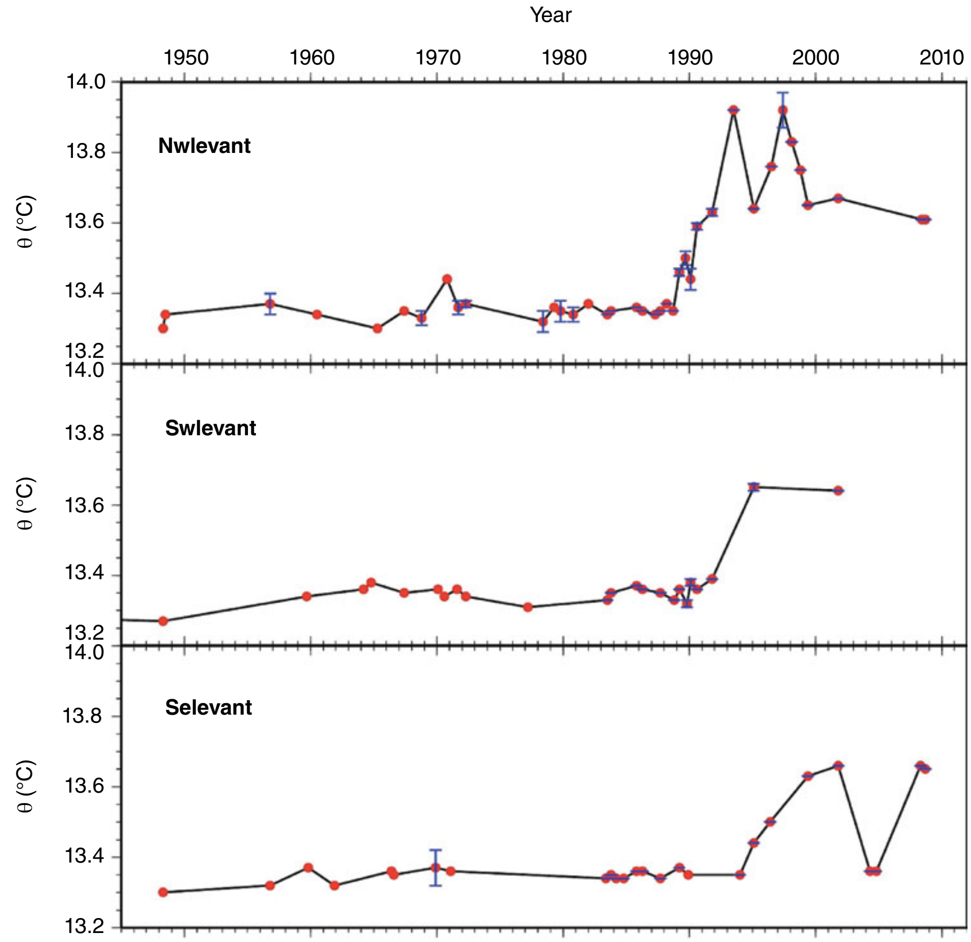

Figure 7.13. Potential temperature θ in the 1900–2100-m depth level in the (a) northwestern, (b) southwestern, and c) southeastern Levantine subdomains. For color detail, please see color plate section.

of Crete, that the stronger EMT signal is conveyed to the Levantine Basin. Since the other straits connecting the Aegean Sea to the eastern Mediterranean are shallower, notably the Antikithira Strait with 560 m sill depth, it is confirmed by the above review of properties in Figures 7.11 and 7.12 that the main outflow route of dense water out of the Cretan Sea is the Kasos Strait, confirming results from the earlier studies [*Roether at al.*, 2007].

The behavior at 2-km depth is different. In the northwest Levantine area adjoining the Kasos Strait (Figure 7.13a), a large temperature signal of 0.6°C is again the largest rise observed among the different subdomains at this depth. A stepwise increase of temperature of about 0.35°C marking the arrival of the EMT signal in the southwest Levantine region (Figure 7.13b) follows closely the northwest region, while in the southeast Levantine, the peak values are reached much later at the end of the 1990s (Figure 7.13c).

Now comparing the Ionian Basin subdomains at 2-km depth, the northeastern Ionian box stands out (Figure 7.14a) indicating a stepwise response with superposed oscillations reaching an amplitude of about 0.5°C in 1993. Smaller amplitude temperature steps of 0.2°C are found at the other subdomains, but with later arrival times of the peak change in about 1995 in the northwest Ionian (Figure 7.14b) and southeast Ionian (Figure 7.14c), and in1998 in the central Ionian Sea (Figure 7.14d).

The above observations suggest direct influence of the EMT on the northwestern Levantine Basin area, from where the anomaly spreads to the southern Levantine Basin and the Ionian Sea. The presence of a large anomaly only in the northwest Levantine area adjacent to the Cretan Sea at 1-km depth (Figures 7.11 and 7.12) confirms the outflow from Kasos Strait at this depth. At the deeper level of 2 km (Figures 7.13 and 7.14), which is more representative of the core of the CDW outflow in the Levantine Basin, the source driven anomaly is present at all subdomains with reduced amplitude and with delays. Due to the basin's size and topographic constraints (obstacles imposed by sea mounts), the EMT

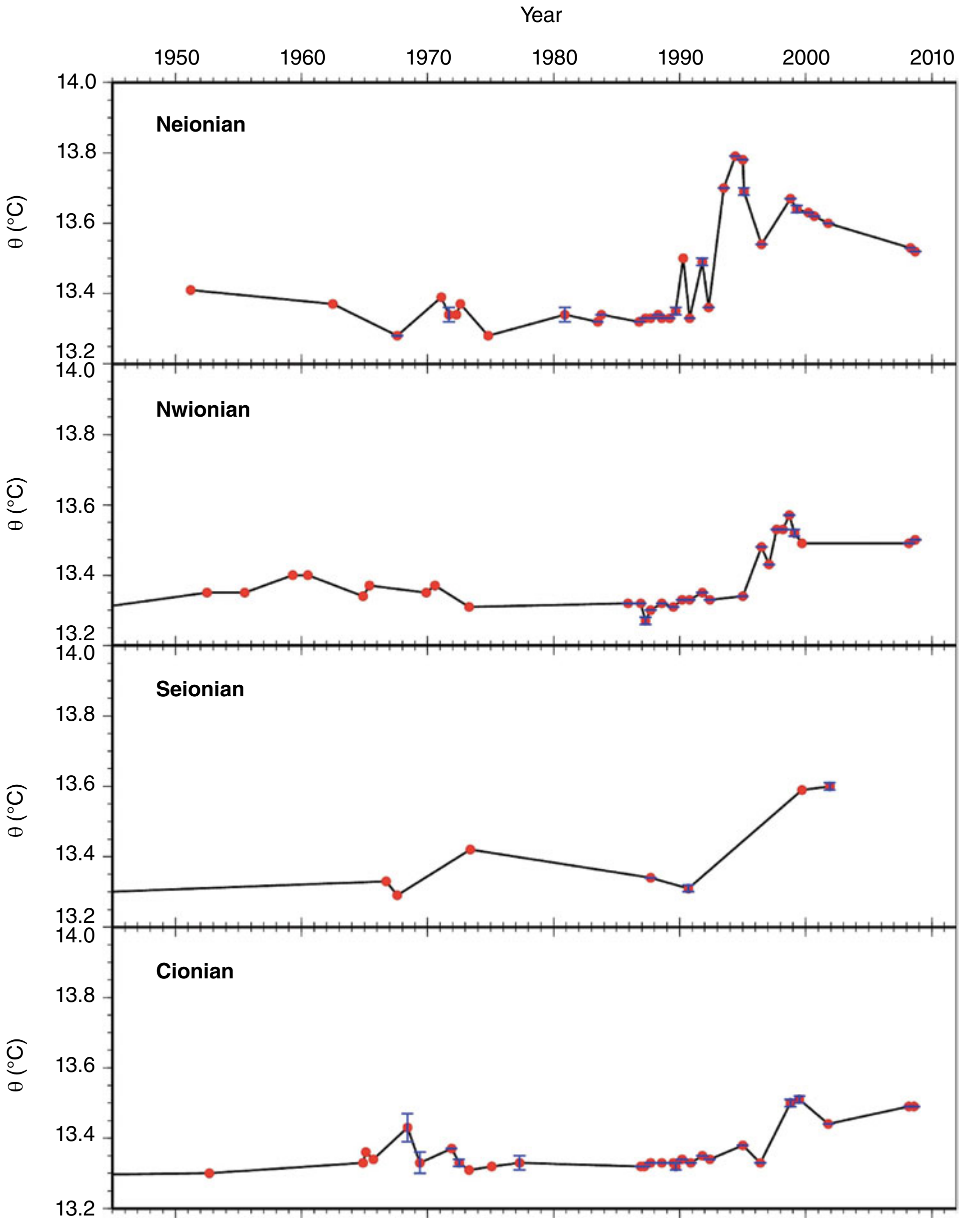

Figure 7.14. Potential temperature θ in the 1900–2100-m depth level in the (a) northeastern, (b) northwestern, (c) southeastern, and (d) central Ionian subdomains. For color detail, please see color plate section.

signal arrives at the southeast Levantine area with a delay of a few years. The origin of outflow in the northwest Levantine area near Kasos Strait at 1 km and the existence of an anomaly of similar amplitude only at 2-km depth in the northeastern Ionian area near Antikithira Strait, with later arrivals elsewhere, confirm the outflow scheme proposed by *Roether et al.* [2007] in his Figure 14: the dense water outflows from Kasos Strait and encircling the deep Hellenic Trench south of Crete arrives in the Ionian Sea, while its southward extension recirculates to both basins along the southern coast after overflowing the eastern Mediterranean Ridge.

Analyses based on the horizontal distributions of properties at any particular time are probably not justified for a historical profiles database of uneven spatial and temporal distribution such as ours. However, by averaging the data roughly for the pre and post-EMT periods, 1970–1990 and 1990–2012, respectively, in Figures 7.15a and 7.15b, we attempt to show the main changes between these two periods, again using deep potential temperature at the 2-km depth layer as tracer.

While the pre-EMT period shows lower temperatures in the Ionian and Levantine basins clearly differentiated from those in the Cretan Sea in Figure 7.15a, the spreading of the warmer and more saline water from the Cretan Sea out into the adjacent basins in the post-EMT period (Figure 7.15b) modifies the deep-water properties throughout the entire area of the Levantine and Ionian basins, with the influence spreading from Kasos Strait through the paths identified above.

7.5. SIMPLE STATISTICS

The number of stations and observation points (scans) in a depth range, and the computed mean and standard deviation and trends computed for the full length of the observation period in each of the maxin subbasins of the eastern Mediterranean are given in Table 7.1.

It is interesting to note that the highest deep salinities and densities occur in the Aegean Sea in the observed period, although partially compensated by potential temperature values slightly higher than the other regions. The coldest deep waters at a given depth interval occur in the Adriatic Sea, with density at 1-km depth remaining higher than the deep Ionian and Levantine sea waters at 4-km depth. Still the highest density occurs in the Aegean Sea, exceeding that of the Adriatic Sea.

Table 7.1 also provides trends in the observed data, calculated by fitting regression lines to the data. Long-term trends appear in the observation periods, including transients and stepwise increases imposed by the EMT in the last two decades. In all the basins, there is a positive trend in all variables at the deeper levels, which is a result of the increases in salinity partially compensated by increased potential temperature. The highest temperature trend partly compensating the salinity increase appears in the Levantine Basin deep waters where the density trend is the lowest. A relatively higher trend in density occurs in

(a)

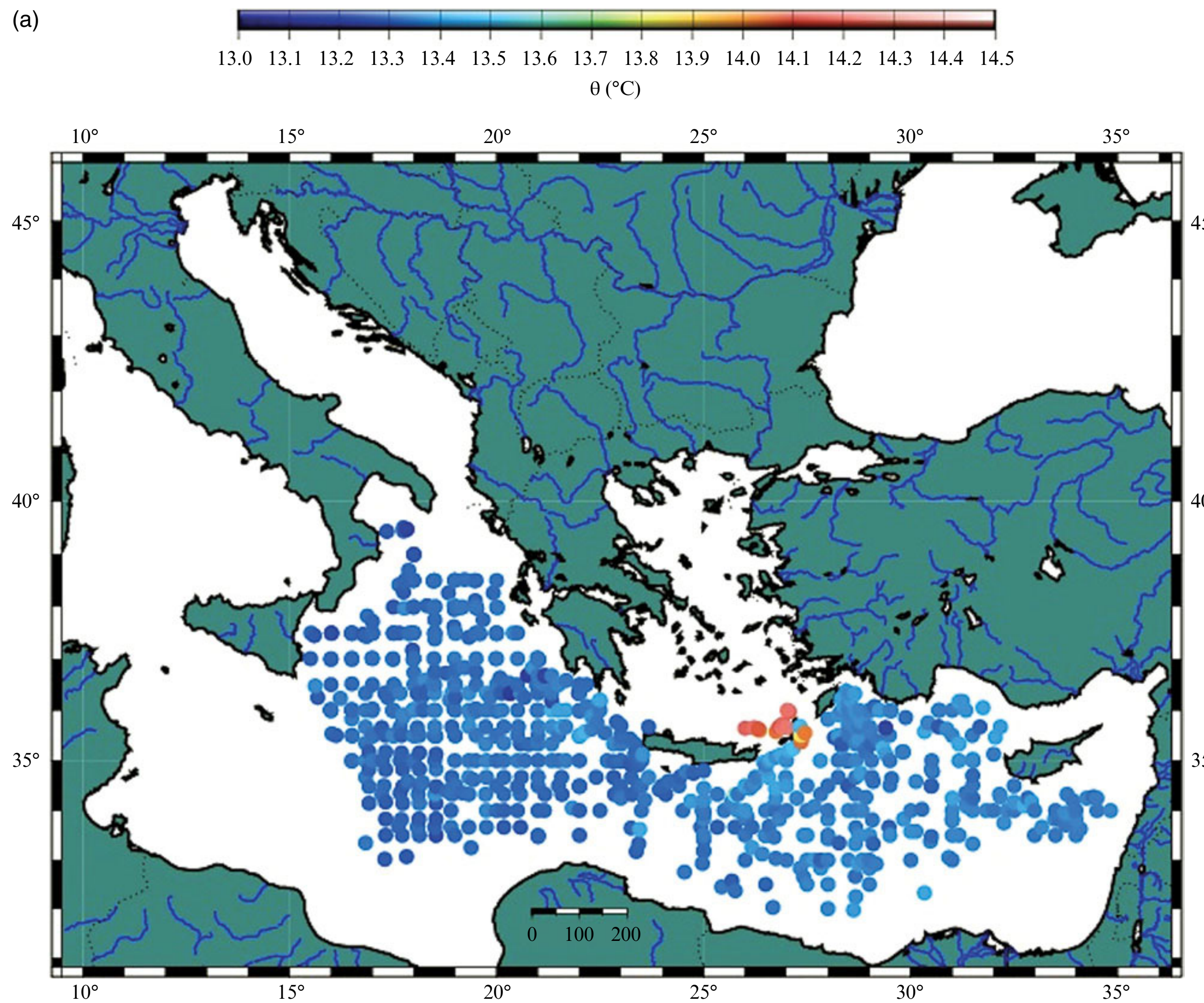

Figure 7.15. Temperature at 1900–2100-m depth interval binned and averaged at 0.1° x 0.1° latitude-longitude intervals during the a) 1970–1990 and

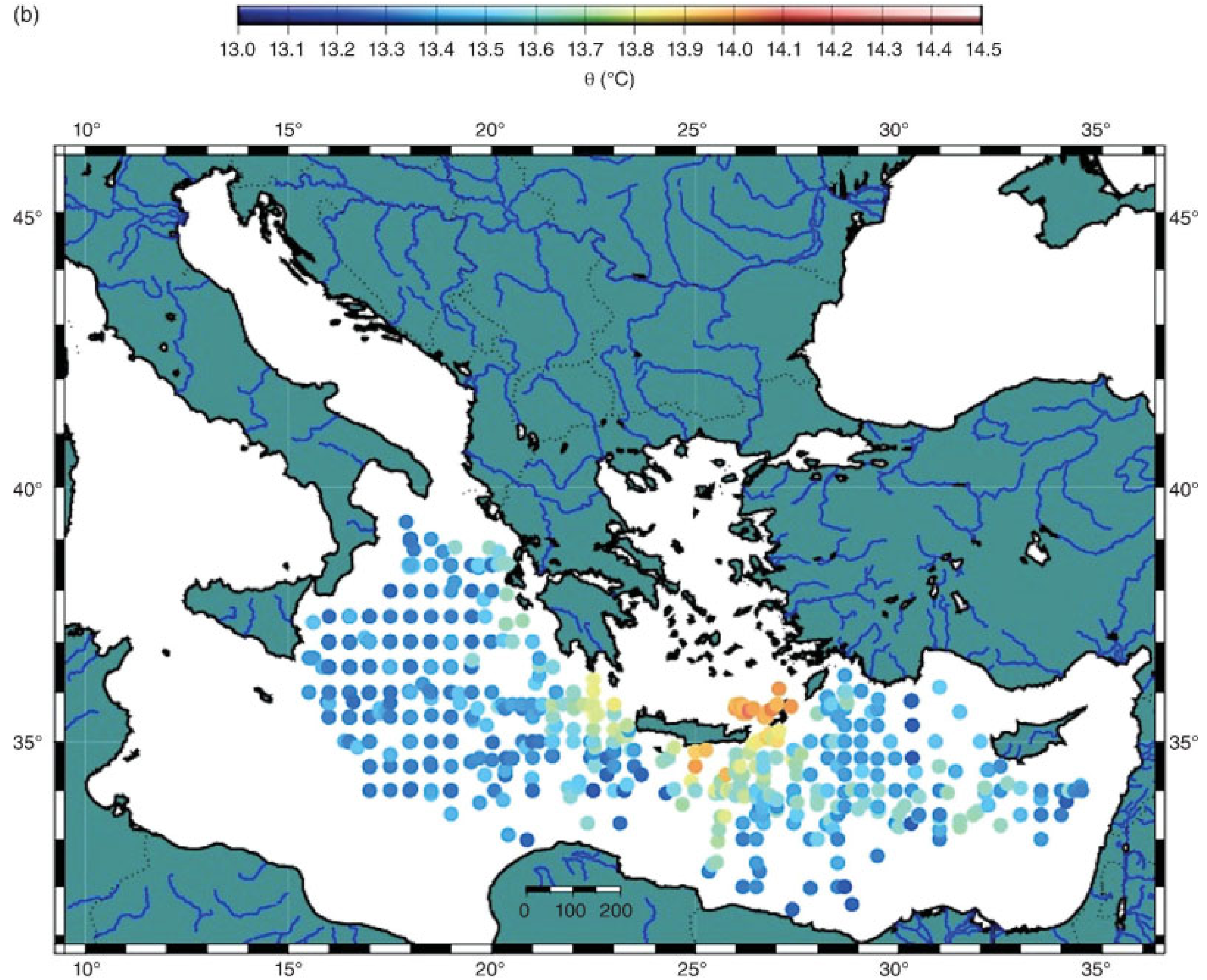

Figure 7.15. (continued) b) 1990–2012 periods. For color detail, please see color plate section.

the Ionian Sea. The highest increase in density occurs in the deep waters of the Aegean and Adriatic seas, where it is associated with cooling effects, with a higher rate in the Aegean Sea.

7.6. DISCUSSION AND CONCLUSIONS

Apart from the very long-term changes, decadal variability is observed to dominate the temporal evolution of the deep waters. It is also observed that the Eastern Mediterranean Transient (EMT) stands as the most extraordinary deep-water episode, while other interdecadal changes of varying strength are predominantly detected in certain areas of the eastern Mediterranean. The largest interdecadal variability is observed in the Aegean and Adriatic basins, where changes are continuously observed during the second half of the last century. An abrupt increase of salinity and density with an associated drop in temperature in the Aegean Basin marks the EMT starting in the early 1990s. In the deep Levantine Basin, the EMT event starts at the same time, particularly after the 1992–1993 cooling event, but lasts throughout the 2000s for about two decades, with stepwise increases in temperature, salinity, and density, attributed to cascading out of the southern Aegean Sea into the adjacent area. In the deep Levantine and Ionian basins, salinity changes dominate the interdecadal variability most of the time. Yet potential temperature proves to be a useful tool to trace these variations, allowing the construction of a basic description of the changes, especially in relation to the EMT. The evolution of the eastern Mediterranean deep-water characteristics suggests a strong interaction between the various subbasins.

The evolution history some years past the EMT can be found in the later literature, showing that the density of the

Table 7.1. Trends in water properties at selected depth intervals in the selected subdomains of the eastern Mediterranean Sea (1948–2010).

Depth Interval (m)–Region	Number of averaged		Potential temperature		Salinity		Potential density	
	stations	scans	mean ± std dev (°C)	trend (10^{-3} °C /yr)	mean ± std dev	trend (10^{-3} /yr)	mean ± std dev (kg/m^3)	trend (10^{-3} kg /m^3/yr)
Adriatic Sea								
0450– 0550	1627	84450	13.41±0.25	1.26	38.72±1.28	1.67	29.18±0.22	1.07
0900– 1100	433	14835	13.04±0.18	−2.33	38.67±0.42	1.53	29.23±0.14	1.66
Aegean Sea								
0450– 0550	2699	70225	14.01±0.51	−0.35	38.96±0.65	2.41	29.25±0.25	1.97
0900– 1100	926	49184	13.89±0.39	4.75	38.98±0.62	2.40	29.29±0.19	0.80
1900– 2100	91	5570	14.03±0.09	−3.98	39.02±0.25	5.16	29.29±0.17	4.83
Levantine Sea								
0450– 0550	7575	290072	13.99±0.32	−2.29	38.92±2.99	−0.22	29.09±1.53	0.29
0900– 1100	5978	332038	13.56±0.32	1.97	38.79±1.12	0.43	29.09±1.93	−0.05
1900– 2100	1748	65806	13.46±0.07	6.33	38.72±0.53	2.30	29.18±0.84	0.40
2900– 3100	112	6125	13.59±0.20	8.75	38.78±0.21	2.77	29.20±0.24	0.40
3900–4100	15	968	13.62±0.12	8.23	38.82±0.15	1.94	29.21±0.10	0.30
Ionian Sea (10273 stations)								
0450– 0550	6014	156955	13.90±0.23	−0.62	38.81±1.08	0.86	29.14±0.30	0.78
0900– 1100	3993	204853	13.57±0.28	0.44	38.67±2.57	0.58	29.15±0.53	0.36
1900– 2100	1982	112464	13.40±0.38	4.20	38.71±0.59	1.82	29.18±0.61	0.45
2900– 3100	552	46314	13.33±0.18	3.23	38.70±0.88	1.70	29.20±1.09	0.62
3900–4100	47	3270	13.40±0.17	2.32	38.73±0.24	1.72	29.20±0.18	0.79

deep water in the Cretan Sea has been decreased back to normal values after the trigger event of the EMT, but the deep water characteristics in the northwestern Levantine Sea region have been shown to survive long after the event [e.g., *Theocharis et al.*, 1999; *Kovačević et al.*, 2012].

Although a description of the climate variability aspects would add significantly to a more basic understanding of the observed deep-sea variability of the eastern Mediterranean, we have excluded the related discussion in this paper, keeping such analyses for future studies. There is already a number of studies on the climatic effects, not fully cited here. The Mediterranean response to climate forcing is rather complex. A synthetic discussion of the climate variability effects and a description of the EMT have been attempted by *Lionello et al*. [2006], among others. Yet, it appears still quite complicated to define how the surface effects are transmitted to deep water by either convective events or lateral fluxes and cascading.

A significant degree of synchronism, possibly imposed by large-scale controls, is often found between the Levantine, Black ,and Caspian seas [*Özsoy*, 1999], implying relationships with the Southern Oscillation (SO) in some years (e.g., 1982–83, 1986–87, the 1990s) or the North Atlantic Oscillation (NAO) in others (1983, 1986–87, 1989–90, 1992–93). Later, principal components analyses performed by *Gündüz and Özsoy* [2005] showed a greater influence of the North Sea Caspian Pattern (NCP) in the Levantine-Aegean-Black seas region compared to the NAO playing a greater role in the western Mediterranean. Especially in the Aegean Sea region, air temperature and surface heat fluxes were very strongly correlated with the NCP dipole pattern during the years 1964, 1975–1976, and 1992–1993. Some of these signals are evident in the analyses performed here. But again, the details and cause-and-effect relationships would probably be better exposed by continuing analyses and modeling efforts.

REFERENCES

Androulidakis, Y. S., V. H. Kourafalou, Y. N. Krestenitis, and V. Zervakis (2012), Variability of deep water mass characteristics in the North Aegean Sea: The role of lateral inputs and atmospheric conditions, *Deep-Sea Res., I 67*, 55–72.

Ashkenazy, Y., P. H. Stone, and P. Malanotte-Rizzoli (2011), Box modeling of the eastern Mediterranean Sea, *Physics A*, *391*, 1519–1531.

Beuvier, J., F. Sevault, M. Herrmann, H. Kontoyiannis, W. Ludwig, M. Rixen, E. Stanev, K. Béranger, and S. Somot (2010), Modeling the Mediterranean Sea interannual variability during 1961– 2000: Focus on the eastern Mediterranean Transient, *J. Geophys. Res.—Oceans*, *115*, C08017, doi:10.1029/2009JC005950.

CIESM (2008), *Toward an integrated system of Mediterranean marine observatories*, No. 34 in CIESM Workshop Monographs, ed. F. Briand, Monaco.

CIESM (2011), *Designing Med-SHIP: A program for repeated oceanographic surveys*, No. 43 in CIESM Workshop Monographs, ed. F. Briand, Monaco.

El-Gindy, A. H., and S. H. S. El-Din (1986), Water masses and circulation patterns in the deep layer of the eastern Mediterranean, *Oceanologica Acta*, *9*, 239–248.

Emery, W. J., and R. E. Thompson (2001), *Data Analysis Methods in Physical Oceanography*, 2 ed., Elsevier Science.

Gačić, M., G. L. E. Borzelli, G. Civitarese, V. Cardin, and S. Yari (2010), Can internal processes sustain reversals of the ocean upper circulation? The Ionian Sea example, *Geophys. Res. Lett.*, *37*, L09608, doi:10.1029/2010GL043216.

Gertman, I. F., N. Pinardi, Y. Popov, and A. Hecht (2006), Aegean Sea water masses during the early stages of the eastern Mediterranean Climatic Transient (1988– 1990), *Journal of Physical Oceanography*, *36*, 1841–1859.

Gündüz, M., and E. Özsoy (2005), Effects of the North Sea Caspian pattern on surface fluxes of Euro-Asian-Mediterranean seas, *Geophys. Res. Lett.*, *32*, 21, doi: 10.1029/2005GL024315.

Hecht A., and I. Gertman (2001), Physical features of the eastern Mediterranean resulting from the integration of POEM data with Russian Mediterranean cruises, *Deep Sea Research, Part I*, *48*/8, 1847–1876.

Hieke, W., P. Halbach, M. Türkay, and H. Weikert, eds. (1994), Mittelmeer 1993, Cruise No. 25, 12 May–20 August 1993, METEOR-Berichte, Universitaet Hamburg, 94–3, 256 pp.

Hoepffner, N., ed. (2006), *Marine and Coastal Dimension of Climate Change in Europe*, A report to the European Water Directors, European Commission, Directorate-General, Joint Research Center, Institute for Environment and Sustainability.

Josey, S. A. (2003), Changes in the heat and freshwater forcing of the eastern Mediterranean and their influence on deep-water formation, *J. Geophys. Res.—Oceans*, *108*, 3237, doi:10.1029/2003JC001778.

Josey, S. A., S. Somot, and M. Tsimplis (2011), Impacts of atmospheric modes of variability on Mediterranean Sea surface heat exchange, *J. Geophys. Res.*, *116*, C02032, doi:10.1029/2010JC006685.

Klein, B., W. Roether, D. Manca, D. Bregant, V. Beitzel, V. Kovacevic, and A. Luchetta (1999), The large deep-water transient in the eastern Mediterranean, *Deep Sea Res.*, *46*, 371–414.

Kontoyiannis, H., E. Balopoulos, A. Pavlidou, O. Gotsis-Skretas, G. Asimakopoulou, E. Papageorgiou, and A. Iona (2005), The hydrodynamics and biochemistry of the Cretan Straits (Antikithira and Kassos Straits) revisited in the period June/1997–May/1998, *Journal of Marine Systems*, *53*, 37–57.

Kovačević, V., B. B. Manca, L. Ursella, K. Schroeder, S. Cozzi, M. Burca, E. Mauri, R. Gerin, G. Notarstefano, and D. Deponte (2012), Water mass properties and dynamic conditions of the eastern Mediterranean in June 2007, *Progress in Oceanography*, *104*, 59–79.

Lacombe, H., and P. Tchernia (1960), Quelques traits genéraux de l'hydrologie Mediterranéene, *Cahiers Océanographiques*, 20(8), 528–547.

Lascaratos A., and K. Nittis, (1998), A high resolution 3-D numerical study of intermediate water formation in the Levantine Sea, *J. Geophys. Res.*, *13*, 18497–18511.

Lascaratos, A., W. Roether, K. Nittis, and B. Klein (1999), Recent changes in deep ocean formation and spreading in the eastern Mediterranean Sea, *Prog. Oceanogr.*, *44*, 5–36.

Lionello, P., P. Malanotte-Rizzoli, and R. Boscolo, eds. (2006), *Mediterranean Climate Variability*, Elsevier Science.

LIWEX Group (2003), The Levantine intermediate water experiment (LIWEX) group: Levantine basin—a laboratory for multiple water mass formation processes, *J. Geophys. Res.*, *198*, doi:10.1029/2002JC001643.

Malanotte-Rizzoli, P., and A. Hecht (1988), Large-scale properties of the eastern Mediterranean: A review, *Oceanol. Acta*, *11*, 323–335.

Malanotte-Rizzoli, P., B. Manca, M. d'Alcala, A. Theocharis, S. Brenner, G. Budillon, and E. Özsoy (1999), The eastern Mediterranean in the 80s and in the 90s: The big transition in the intermediate and deep circulations, *Dyn. Atmos. Oceans*, *29*, 365–395.

Malanotte-Rizzoli, P., B. Manca,, S. Marullo, M. d'Alcala, A. Theocharis, A. Bergamasco, G. Budillon, E. Sansone, G. Civitarese, F. Conversano, I. Gertman, B. Herut, N. Kress, S. Kioroglou, H. Kontoyannis, K. Nittis, B. Klein, A. Lascaratos, M. A. Latif, E. Özsoy, A. R. Robinson, R. Santoleri, D. Viezzoli, and V. Kovacevic (2003), The Levantine Intermediate Water Experiment (LIWEX) Group: Levantine Basin—laboratory for multiple water mass formation processes, *J. Geophys. Res.*, *108* (C9), 8101.

Malanotte-Rizzoli, P., and the Pan-Med Group (2012), Physical forcing and physical/biochemical variability of the Mediterranean Sea: A review of unresolved issues and directions of future research, Report of the Workshop Variability of the Eastern and Western Mediterranean circulation and Thermohaline Properties: Similarities and Differences, Rome, November 7–9, 2011, 48 pp.

Miller, A. R. (1974), Deep convection in the Aegean Sea, in *Processus de Formation des Eaux Oceaniques Profondes*, Colloques Internationaux du C. N. R. S. 215.

Nielsen, J. (1912), Hydrography of the Mediterranean and adjacent waters, in *Report of the Danish Oceanographic Expedition 1908–1910 to the Mediterranean and Adjacent Waters*, Vol. *1*, pp. 72–191.

Nittis, K., A. Lascaratos, and A. Theocharis (2003), Dense water formation in the Aegean Sea: Numerical simulations during the Eastern Mediterranean Transient, *J. Geophys. Res.*, *108* (C9), PBE 21, doi:10.1029/2002JC001352.

Ovchinnikov, I. M., and A. Plakhin (1984), Formation of the intermediate waters of the Mediterranean Sea in the Rhodes Cyclonic Gyre, *Oceanology*, *24*, 317–319.

Ovchinnikov, I. M., Y. I. Popov, and I. F. Gertman (1990), A study of the deep water formation in the eastern Mediterranean Sea, *Oceanology*, *30*, 6, 1039–1041.

Özsoy, E. (1999), Sensitivity to global change in temperate Euro-Asian seas (the Mediterranean, Black Sea and Caspian Sea): A review, in *The Eastern Mediterranean as a Laboratory Basin for the Assessment of Contrasting Ecosystems*, pp. 281–300, ed. P. Malanotte-Rizzoli and V. N. Eremeev, NATO Science Series 2, Environmental Security, 51, Kluwer Academic Publishers, Dordrecht.

Özsoy, E., A. Hecht, and Ü. Ünlüata (1989), Circulation and hydrography of the Levantine Basin: Results of POEM-coordinated experiments 1985–1986, *Prog. Oceanogr.*, *22*, 125–170.

Özsoy, E., A. Hecht, Ü. Ünlüata, S. Brenner, H. İ. Sur, J. Bishop, M. A. Latif, Z. Rozentraub, and T. Oğuz (1993), A synthesis of the Levantine Basin circulation and hydrography, 1985–1990, *Deep-Sea Res.*, *40*, 1075–1119.

Özsoy, E., and M. A. Latif (1996), *Climate Variability in the Eastern Mediterranean and the Great Aegean Outflow Anomaly*, International POEM-BC/MTP Symposium, Molitg les Bains, France, 1–2 July 1996, pp. 69–86.

Özsoy, E., Ü. Ünlüata, T. Oğuz, M. A. Latif, A. Hecht, S. Brenner, J. Bishop, and Z. Rozentroub (1991), A review of the Levantine Basin circulation and its variabilities during 1985–1988, *Dyn Atmos. Oceans*, *15*, 421–456.

Pinardi, N., and E. Masetti (2000), Variability of the large-scale general circulation of the Mediterranean Sea from observations and modelling: A review, *Palaeogeography, Palaeoclimatology, Palaeoecology*, *158*, 153–173.

Plakhin, Ye. A. (1972), Vertical winter circulation in the Mediterranean, *Oceanology*, *12*, 344–351.

POEM Group (A. R. Robinson, P. Malanotte Rizzoli, A. Hecht, A. Michelato, W. Roether, A. Theocharis, Ü. Ünlüata, N. Pinardi, A. Artegiani, A. Bergamasco, J. Bishop, S. Brenner, S. Christianidis, M. Gačić, D. Georgopoulos, M. Golnaraghi, M. Hausmann, H. G. Junghaus, A. Lascaratos, M. A. Latif, W. G. Leslie, C. J. Lozano, T. Oğuz, E. Özsoy, E. Papageorgiou, E. Paschini, Z. Rozentroub, E. Sansone, P. Scarazzato,R. Schlitzer, G. C. Spezie, E. Tziperman, G. Zodiatis, L. Athanassiadou, M. Gerges, M. Osman) (1992), General circulation of the eastern Mediterranean, *Earth-Sci. Rev.*, *32*, 285–309.

Pollak, M. I. (1951), The sources of deep-water in the eastern Mediterranean Sea, *Journal of Marine Research*, *10*, 128–152.

Press, W. H., S. A. Teukolsky, W. T. Vetterling, and B. P. Flannery (2007), *Numerical Recipes*, 3 ed., Cambridge University Press.

Roether, W., and R. Schlitzer (1991), Eastern Mediterranean deep-water renewal on the basis of chlorofluoromethane and tritium data, *Dyn. Atmos. Oceans*, *15* (3–5), 333–354.

Roether, W., B. Manca, B. Klein, D. Bregant, D. Georgopoulos, V. Beitzel, V. Kovacevic, and A. Lucchetta (1996), Recent changes in eastern Mediterranean deep waters. *Science*, *271*, 333–335.

Roether W., B. Klein, B. B. Manca, A. Theocharis, and S. Kioroglou (2007), Transient Eastern Mediterranean deep waters in response to the massive dense-water output of the Aegean Sea in the 1990s, *Progr. Oceanogr.*, *74*, 540–571, doi:10.1016/j.pocean.2007.03.001.

Samuel, S., K. Haines, S. Josey, and P. Myers (1999), Response of the Mediterranean sea thermohaline circulation to observed changes in the winter wind stress field in the period 1993, *J. Geophys. Res. Oceans*, *104*, 7771–7784.

Sayın, E., and Ş. T. Beşiktepe (2010), Temporal evolution of the water mass properties during the Eastern Mediterranean Transient (EMT) in the Aegean Sea, *J. Geophys. Res.*, *115*, C10025, doi:10.1029/2009JC005694.

Schlitzer, R., W. Roether, H. Oster, H. Junghans, H. Hausmann, H. Johannsen, and A. Michelato (1991), Chlorofluoromethane and oxygen in the eastern Mediterranean, *Deep Sea Res.*, *38*, 1531–1551.

Stratford, K., and K. Haines(2002), Modelling changes in Mediterranean thermohaline circulation 1987–1995 *J. Mar. Syst.*, *33*, 51–62.

Sur, H., E. Özsoy, and Ü. Ünlüata (1993), Simultaneous deep and intermediate depth convection in the Northern Levantine Sea, winter 1992, *Oceanol. Acta*, *16*, 33–43.

Theocharis, A., and D. Georgopoulos (1993), Dense water formation over the Samothraki and Lemnos plateaux in the North Aegean Sea (eastern Mediterranean Sea), *Continental Shelf Research*, *l3*(S-9), 919–939.

Theocharis, A., K. Nittis,, H. Kontoyiannis,, E. Papageorgiou, and E. Balopoulos (1999), Climatic changes in the Aegean influence the eastern Mediterranean thermohaline circulation (1986–1997), *Geophys. Res. Lett.*, *26*, 1617–1620.

Theocharis, A., B. Klein, K. Nittis, and W. Roether (2002), Evolution and status of the Eastern Mediterranean Transient (1997–1999), *Journal of Marine Systems*, *33–34*, 91–116.

Vervatis, V., S. Sofianos, and A. Theocharis (2011), Distribution of the thermohaline characteristics in the Aegean Sea related to water mass formation processes (2005–2006 winter surveys), *J. Geophys. Res.*, *116*, C09034, doi:10.1029/2010JC006868.

Wu, P., K. Haines, and N. Pinardi (2000), Toward an understanding of deep-water renewal in the eastern Mediterranean, *J. Phys. Oceanogr.*, *30*, 443–458.

Wüst, G. (1961), On the vertical circulation of the Mediterranean Sea, *J. Geophys. Res.*, *66*, 3261–3271.

Zervakis, V., D. Georgopoulos, and P. Drakopoulos (2000), The role of North Aegean in triggering the recent eastern Mediterranean climatic changes, *J. Geophys. Res.*, *105*, 26103–26116.

Zervakis, V., and D. Georgopoulos (2002), Hydrology and circulation in the North Aegean (eastern Mediterranean) throughout 1997 and 1998, *Mediterranean Marine Science*, *3*, 5–19.

Zervakis, V., D. Georgopoulos, and P. G. Drakopoulos (2000), The role of the North Aegean in triggering the recent eastern Mediterranean climatic changes, *J. Geophys. Res.*, *105* (C11), 103–116.

Zervakis, V., E. Krasakopoulou, D. Georgopoulos, and E. Souvermezoglou (2003), *Vertical Diffusion and Oxygen Consumption during Stagnation Periods in the Deep North Aegean*, Deep-Sea Res., Part I, Oceanographic Research Papers. *50*, 53–71.

Zodiatis, G. (1992), On the seasonal variability of the water masses circulation in the NW Levantine Basin-Cretan Sea and flows through the eastern Cretan Arc Straits, *Ann. Geophysicae*, *10*, 12–24.

Zodiatis, G. (1993). Water mass circulation between the SE Ionian–W Cretan basins through the western Cretan Arc Straits, *Bollettino di Oceanologia Teorica ed applicata*, *11*, 1, 61–75.